Journal of Structural Dynamics, 2, (pp. 51-81) 2023
A unified framework for corotational flexible multibody system dynamics formulations

Journal of Structural Dynamics

A unified framework for corotational flexible multibody system dynamics formulations

Andreas Zwölfer*[1] and Johannes Gerstmayr†[2]

[1] *Technical University of Munich, TUM School of Engineering and Design, Department of Mechanical Engineering, Chair of Applied Mechanics, Boltzmannstr. 15, Garching, Germany*
[2] *University of Innsbruck, Department of Mechatronics, Technikerstr. 13, Innsbruck, Austria*

Abstract

Corotational formulations play an important role for flexible multibody dynamics systems, because they reflect the nature of many technical systems undergoing arbitrarily large rigid body motions but small deformations within each body.

This paper defines flexible multibody dynamics and corotational formulations in this context. Furthermore, the "ingredients" and workflow of a flexible multibody dynamics simulation are briefly addressed for the reader less familiar with the topic. This part also points to major review papers and textbooks in the field, and embeds the unified formulations in the literature.

The paper's main part presents state-of-the-art corotational flexible multibody dynamics formulations in a systematic and unified way. In this formulation part, the standard integral-based floating frame of reference formulation with modal reduction and with the conventionally employed lumped mass approximation is presented, and its drawbacks highlighted. Then, the so-called nodal-based, i.e., space-wise discretized, equations of motion are presented for several up-to-date nodal-displacement-based formulations within a unified framework. This approach clearly shows the equivalence of the presented formulations, and highlights the fact that the formulations differ only in the choice of degrees of freedom. Moreover, this contribution also intends to reduce the information and complexity within the scientific literature, since this unified framework allows the derivation of these formulations with significantly less effort.

Keywords: Flexible multibody system dynamics; corotational formulation; floating frame of reference formulation; absolute coordinate formulation; generalized component mode synthesis; flexible natural coordinate formulation

Received on December 14, 2021, Accepted on June 5, 2023, Published on June 12, 2023

Contents

*andreas.zwoelfer@tum.de
†johannes.gerstmayr@uibk.ac.at

1 Introduction

1.1 Organization of this paper

Sect. 1 defines flexible multibody dynamics and corotational formulations in this context. Furthermore, the "ingredients" and workflow of a flexible multibody dynamics simulation are addressed for readers less familiar with the topic. This part also points to major review papers and textbooks and embeds the unified formulations in the literature.

As the paper's main objective, Sect. 2 provides a state-of-the-art description of the equations of motion of corotational flexible multibody dynamics formulations and shows that despite the fact that conventional formulations are accompanied by cumbersome derivations, filling pages of books/papers, these equations of motion can be derived in a few lines using appropriate notation and operations. This is enabled by a unification framework, which requires the definition of generalized coordinates, mappings between nodal quantities and generalized coordinates, and associated Jacobians. This enables us to unify the floating frame of reference formulation (FFRF), component mode synthesis (CMS)-FFRF, absolute coordinate formulation (ACF), generalized component mode synthesis (GCMS), and flexible natural coordinates formulation (FNCF).

1.2 Flexible multibody system dynamics defined

The growing complexity and demanded performance of mechanical systems we are facing, force engineers to take flexibility of system parts into account. Yet, classical nonlinear finite element methods are often limited to a moderate number of generalized coordinates and/or short simulation periods because of computational efficiency reasons. However, what we refer to as flexible flexible multibody dynamics simulations are powerful and efficient tools to realistically model real-world, multiple-component devices in their intended operating environment, and show potential for real-time applications.

Flexible multibody dynamics refers to computational strategies employed to determine long time histories of motion, deformation, strain, and stress of a group of interconnected rigid and deformable components, which are subjected to large rigid body translations and rotations due to applied forces, constraints, contacts, and initial conditions [1, 2].

Based on the degree of flexibility taken into account, one can distinguish between three classes of multibody systems[1]. The simplest are rigid multibody systems, which consist exclusively of rigid bodies. However, flexibility may be represented through flexible bushings and joints, which connect the rigid bodies, and therefore, allow localized deformation at the connection points. The next level of complexity is reached with so-called linearly-elastic multibody systems, where the bodies' flexibility is taken into account, but under the assumptions of small body-level deformations and strains as well as a linear constitutive law. This class still allows efficient simulations of three-dimensional bodies with appropriate modal reduction. Finally, we encounter nonlinearly-elastic multibody systems as

[1] Note that all three classes are characterized by nonlinear equations of motion and that they often appear simultaneously within one simulation, since only the critical parts are modeled as elastic bodies and other parts are kept rigid to keep the computational complexity to a minimum.

soon as we drop the assumptions of small deformations/strains and/or a linear constitutive law; such simulations are often limited to structural elements, such as beams and shells, due to computational limitations. [3]

Typical examples of systems analyzed via flexible multibody dynamics simulations are ground/aerial vehicles, robots, the human/animal body, machines/mechanisms, sporting goods, and particle systems.

1.3 Reviews and books

There is a vast and growing body of literature on the dynamics of flexible multibody systems. A selection of review papers devoted to – or including topics of – the field is listed chronologically below:

- Huston in 1981 [4]
- Huston in 1991 [5, 6]
- Schiehlen in 1997 [7]
- Shabana in 1997 [1]
- Bremer in 1999 [8]
- Wasfy & Noor in 2003 [2]
- Eberhard & Schiehlen in 2006 [9]
- Schiehlen in 2006 [10]
- Bauchau & Laulusa in 2008 [11]
- Gerstmayr et al. in 2013 [12]
- Tian et al. in 2018 [13]
- Rong et al. in 2019 [14]
- Rui et al. in 2019 [15]
- Flores in 2021 [16]
- Gufler et al. in 2021 [17]
- Otsuka et al. in 2022 [18]

Also, a selection of textbooks including topics of flexible multibody dynamics are listed chronologically below:

- Huston in 1990 [19]
- Bremer & Pfeiffer in 1992 [20]
- De Jalon & Bayo in 1994 [21]
- Schwertassek & Wallrapp in 1999 [22]
- Géradin & Cardona in 2001 [23]
- Bremer in 2008 [24]
- Pfeiffer in 2008 [25]
- Bauchau in 2011 [3]
- Jain in 2011 [26]
- Simeon in 2013 [27]
- Schiehlen & Eberhard in 2014 [28]
- Seifried in 2014 [29]
- Shabana in 2018 [30]
- Shabana in 2020 [31]

The aforementioned references focus on what we will later (Sect. 1.6 and 2) identify as FFRF [31] and/or formulations tailor-made typically for beam and/or shell elements, such as the absolute nodal coordinate formulation (ANCF) [12, 18] or geometrically exact beam formulation [32]. However, other corotational formulations presented in here are not treated in detail despite their equivalence as established in Sect. 2.3.

1.4 Corotational flexible multibody dynamics formulations defined

This paper focuses on linearly-elastic flexible multibody dynamics as defined in Sect. 1.2; within this class we define corotational formulations as follows:

Definition of corotational flexible multibody dynamics formulations

A corotational flexible multibody dynamics formulation is based on a kinematic description that additively decomposes the total displacement field of a linearly-elastic body into an arbitrarily large rigid body motion and superimposed small deformations.

These assumptions and the underlying kinematics are also cast into equation form in Sect. 2.3.

The importance of corotational formulations is due to their suitability to model bodies undergoing large rigid body motion and small superimposed deformations, i.e., many engineering systems of practical importance, efficiently. Furthermore, the idea of such a splitting of displacements into rigid body motion and deformation is a straightforward and intuitive extension of rigid body dynamics and easy to implement. Therefore, corotational formulations attract researchers and practitioners in academia and industry.

The term corotational was already used in the sixties/seventies by the continuum mechanics / finite element community as mentioned in [33]. The article [33] presents not only a unified framework but also a literature review of corotational finite element formulations in structural dynamics, where the corotational idea in finite element methods is attributed to [34, 35] according to [36]. More recent information of the topic may be also found in [37]. The term is indeed less common in the flexible multibody dynamics community and often contrasted to classical flexible multibody dynamics formulations such as the FFRF [2]. However, the fundamental kinematic assumption of an additive decomposition of the total displacement field into an arbitrarily large rigid body motion and superimposed small deformations is the same [34, 33]. Although, compared to corotational finite element formulations, where each finite element has one moving[2] frame per element, corotational flexible multibody dynamics formulations have one moving frame per body or, at most, per substructure, i.e., a subdivision of one body into multiple parts – hence, small deformations with respect to each substructure may end up representing "larger" deformations on a body level. A moving frame per element is then the extreme case and can, therefore, represent large body-level deformation. Also, corotational finite element formulations are not limited to a linear material law [33]. Felippa & Haugen [33] also mention Fraeijs de Veubeke's work [38] – considered one of the early references of flexible multibody dynamics formulations – trying to use the "rigid-plus-deformational decomposition idea [shadow frame] for an entire structure", i.e., exactly what we also consider the definition of corotational flexible multibody dynamics formulations.

The representatives of corotational flexible multibody dynamics formulations are the FFRF with and without modal reduction, ACF, GCMS, and FNCF, as discussed in more detail in Sect. 1.6 and rigorously in Sect. 2.

1.5 Ingredients of corotational flexible multibody dynamics simulations in a nutshell

The typical "ingredients" necessary to set up a flexible multibody dynamics simulation are;

- □ equations of motion usually with modal reduction;
- □ joints, i.e., inter-body constraints;
- □ loads: forces/torques (applied/elements), contacts;
- □ reference, i.e., intra-body, constraints;
- □ solution procedure.

This paper's main objective is the unification of the equations of motion of corotational flexible multibody dynamics formulations in Sect. 2. The other "ingredients" listed above are not its focus but will be addressed briefly here.

Flexible multibody simulations usually required the reduction of the number of flexible generalized coordinates due to computational efficiency reasons. The well-established component mode synthesis, where the flexible deformation is approximated by a linear combination of component modes is a widely used approach to do so. Any projection-based technique may be employed in corotational flexible multibody dynamics. Modes employed in the reduction basis may include (free-free/fixed-free/fixed) vibration eigenmodes, various different attachment/constraint modes, etc. to obtain, e.g., Craig-Bampton's, Craig-Chang's, Herting's, or Rubin's method, see [39, 40, 41, 42, 43, 44, 45, 46] for details. As an alternative to these techniques, Krylov subspace and balanced truncation methods, which take into account controllability and observability to find a (projection-based) reduction basis, may be employed as well [47, 48, 39].

Joints, i.e., inter-body constraints, e.g., spherical, revolute, prismatic, etc. [23, 49] between bodies are represented as algebraic equations in the system generalized coordinates and enforced [50, 11] typically via Lagrange multipliers. This modeling strategy is often referred to as dependent coordinate approach in contrast to a minimal/joint coordinate approach [51, 52, 53, 54, 55].

Defining joints or loads, such as applied forces/torques, force elements, e.g., springs and dashpots, and contact [16], at single points of flexible bodies may lead to problems, such as unrealistic modeling and/or excessive local deformations. Hence, rigid or interpolation multipoint constraints are employed. In rigid multipoint constraints an interface node set is constrained to follow a master node, while in interpolation multipoint constraints the motion (translation and rotation) of the master node is determined by the average motion of the nodes in the interface set [56, 57]. The master nodes may then be loaded or included in standard joint constraints. The rotation and translation of the master node may be defined from pure displacement-based finite elements (employed in Sect. 2); this reintroduction of rotations is not a problem as these are merely used to define joints and apply loads.

In addition to intra-body constraints related to the rigid body motion, e.g., norm of Euler parameters equals one [58], six (in three dimensions) reference constraints are potentially necessary to remove the rigid body motion from the flexible displacement field in order to remove coordinate redundancy. This process is also referred to as the selection of the moving frame / dynamical axes. It may be achieved by setting as many flexible generalized coordinates as

[2] [33] also mention shadow(-element), ghost(-reference), and phantom as alternative terminology when referring to the rigid-body motion frame.

necessary to zero, and therefore, "attaching the moving frame to these nodes" [59]. The definition may be also based on dynamical concepts, e.g., a so-called Tisserand/Gylden/mean-axis frame associated with zero linear and angular momentum as well as minimum kinetic energy due to body-level deformation [59]. A more detailed treatment of reference constraints may be not only found in [59] but also in earlier works [38, 60]. Reference conditions may also take the geometrical properties of mechanical joints into account [61, 62, 63], be defined using multipoint constraints [64], and lead to large errors if chosen poorly [65].

Because of nonlinear ordinary differential and algebraic constraint equations, the problem is governed by a differential algebraic equation system. Hence, tailor-made solution procedures, typically involving time integration schemes, are necessary, see, e.g., [66, 67, 68, 69, 70, 11, 50, 2, 14].

1.6 Corotational flexible multibody dynamics formulations pre discussion

The equations of motion of corotational flexible multibody systems under focus are usually derived via a straightforward extension of rigid body dynamics, i.e., the kinematic description involves a rigid body translation and rotation part, as in rigid body dynamics, and a deformation term is simply added, see Sect. 2.2 and in particular Eq. (1) as well as Fig. 1 for details. Conventionally the generalized coordinates of a flexible body are then the translation and rotation of the underlying rigid body motion / moving frame as well as local deformation measures. The formulation obtained with these local flexible generalized coordinates is referred to as FFRF.

The FFRF has become standard for modeling corotational flexible multibody systems and is without doubt the most widely-used method and implemented in most commercial software packages, such as RecurDyn [71], Adams [72], Simcenter 3D [73], MotionSolve [74], SIMPACK [75]. Flexible multibody dynamics codes conventionally rely on other codes to provide the information necessary to build the equations of motion of the FFRF, see Sect. 2.2. The workflow is as follows: (i) The geometry is either created in a dedicated computer-aided design software and imported into the finite element code or created in the finite element code directly. (ii) Within the finite element code the data necessary for the flexible multibody dynamics code is generated. (iii) Then, using MSC.ADAMS terminology, the (binary) modal neutral file (*.mnf), which includes

- metadata,
- mesh data (nodal coordinates, element faces, interface nodes),
- mode shapes and eigenvalues,
- units,
- mass and stiffness matrix,
- inertia invariants,
- global mass properties,
- nodal masses and inertias,
- modal preload,
- stress and strain shapes (optional),

exported by the finite element code is imported into the flexible multibody dynamics code where the final model is set up and solved. Hence, no direct access to, e.g., shape functions of the underlying finite element formulation is necessary. This workflow is the same for all the formulations presented within the common framework of Sect. 2.3.

The conventional FFRF is based on so-called inertia shape integrals (see Sect. 2.2.1) over the finite element shape functions [31, 76, 77, 78, 79]. The efficient computation of the these integrals has been topic of interest ever since [80]. Sect. 2.2.3 explains that commercial flexible multibody dynamics codes resort to a lumped mass approximation to circumvent the integral issue and enable the aforementioned workflow. All required matrices may be also be obtained from a standard input data interface [59] which, however, is not needed if the nodal based approach is used, see Sect. 2, especially 2.3.3 and 2.3.4. It is also known that some of the inertia terms play a minor role in certain applications [81] and may be disabled in dedicated software packages to speed up computations.

Term FFRF is not always used in the literature to denote the formulation as defined above. For example; [21] denote the FFRF as the classical moving frame approach; [82] use the term relative nodal coordinate formulation; the robotics/mechanism community, e.g., [83], uses the FFRF, where the equations of motion are projected into the joint space to obtain a minimal (rigid body) coordinate representation, but seemingly does not see the connection to FFRF as the approach is named equivalent rigid-link system and contrasted to the FFRF [83]. However, the term was used at least in the seventies [60], and [31] as well as [22], whose authors made substantial contributions early on to the formulation, use FFRF[3].

As an alternative to FFRF, ACF has been developed [84] in order to perform high-fidelity dynamic simulations of large scale finite element models discretized with volume elements [85], allowing efficient numerical time integration

[3] In his German writings Schwertassek [22] used the term "Methode des bewegten Bezugssystems", which literally translates to "method of the moving reference frame".

due to a constant Jacobian matrix [84]. The formulation behind ACF relies on a corotational linearization of the strain tensor. This provides an efficient alternative to fully nonlinear finite element methods, which would require the assembly of nonlinear forces in every computation step. Furthermore, ACF yields a constant mass matrix in contrast to the FFRF. Note that ACF is considerably different from ANCF [12, 18] employing absolute nodal position and slope vectors as generalized coordinates.

The similarity of ACF and FFRF is that both formulations use a corotationally linearized model for elastic forces [86]. The difference is that the equations of motion and elastic coordinates are defined in the global frame for ACF while the flexible part of FFRF is defined in the local frame. This leads to considerable simplifications in the equations of motion for ACF at the expense that modal reduction becomes more complicated, see GCMS [87, 88, 89] in Sect. 2.3.6. If the same geometrical interpolations and reference frames are used, results are identical for both formulations [86], as is now clear since one formulation may be derived from the other and vice versa [90, 91].

An extension of modal reduction has been proposed by [87] for the planar case and later on extended to three dimensions [88]. To this end, the mode shapes need to approximate the flexible and large rigid body motion of a body. For this reason, the planar approach [87] relied on the idea to use perpendicular mode shapes that represent a conventional mode shape in any rotated state. The three dimensional extension [88], denoted as GCMS, shows the disadvantage of nine generalized mode shapes instead of one as in FFRF. Furthermore, it turned out that in certain cases these generalized mode shapes are linearly dependent [89], which needs to be removed. Nevertheless, the advantage of GCMS is the global approximation of the motion of a flexible body, which can be used for global modal parameterization [92], introduced by [93], in order to perform a reduction of the system as a whole instead of on a body level, or for FNCF [94].

The combination of the advantages of FFRF and GCMS, being the simplicity of elastic respectively inertia forces, has been proposed by [94]. The approach, denoted as FNCF, is based on highly redundant coordinates with additional intra-body constraints. Under certain circumstances, the constraint equations remain quadratic, leading to computationally efficient evaluation of the constraint Jacobian besides the simplistic equation of motion structure.

Other developments regarding corotational flexible multibody dynamics formulations not included in the unified framework of Sect. 2.3 are mentioned briefly below: Cardona & Géradin made significant contributions to corotational flexible multibody dynamics formulations with the so-called superelement approach [95, 96, 97] employing boundary and vibration modes in the reduction basis and positions and rotations of the boundary nodes in the global frame and the internal vibration amplitudes as generalized coordinates. Also, a method has been presented which aims at transforming rigid body and flexible generalized coordinates of the conventional FFRF into absolute interface coordinates, i.e., the core idea of the superelement formulation [95, 96, 97], using Hurty/Craig-Bampton interface modes [98]. The impulse-based formulation of [99] based on FFRF generalized coordinates has been proposed for the modeling of elastic bodies subjected to rigid body motion, which leads to a significant simplification of the equations of motion due to an approximation of the kinetic energy. A two-field formulation has been presented recently by the same authors [100, 101] but without approximating the kinetic energy; nevertheless, by considering the elastic displacement and velocity fields as independent, the kinetic energy may be again uncoupled and simpler equations of motion are obtained, but at the expense of doubling the generalized coordinates.

2 Rigorous treatment of corotational flexible multibody dynamics formulations

2.1 Preliminary remark

It shall be emphasized that the following considerations apply to the most general three-dimensional case, although, the formulations may be, of course, also presented in lower dimensions. The only real restriction is the limitation to displacement-based finite elements as discussed in more detail in Sect. 2.3.2.

Note also that the following treatment deals with the equations of motion of one representative body of the system, only. For the sake of simplicity we omit, e.g., subscripts denoting the body under consideration.

The treatment of constraints is also set aside as their enforcement is not affected by the unified framework. For example, to enforce inter-body constraints, classical multipoint constraints [56] are defined and afterwards coupled via Lagrange multipliers to realize joints [49] known from rigid multibody dynamics. Furthermore, the fact that the unified framework is derived with (translational) displacement-based finite elements does not affect the definition of multipoint constraints since translations and rotations of master nodes are calculated from the translational nodal displacements of node sets; the motions of master nodes are then coupled in the conventional way.

2.2 The conventional floating frame of reference formulation

2.2.1 Inertia-shape integral floating frame of reference formulation

The conventional derivation of the FFRF equations of motion is based on continuum mechanics theory [31]. In the conventional approach, the definition of the continuous position[4] $\boldsymbol{r} \in \mathbb{R}^{3\times1}$ of a material point $\overline{\boldsymbol{x}} \in \mathbb{R}^{3\times1}$ is given by (see Fig. 1)

$$\boldsymbol{r}(\overline{\boldsymbol{x}},t) = \underbrace{\boldsymbol{\tau}(t)}_{\text{translat.}} + \underbrace{\boldsymbol{A}(\boldsymbol{\theta}(t))\,\overline{\boldsymbol{x}}}_{\text{rotation}} + \underbrace{\boldsymbol{A}(\boldsymbol{\theta}(t))\,\overline{\boldsymbol{c}}_{\mathrm{f}}(\overline{\boldsymbol{x}},t)}_{\text{deformation}}, \tag{1}$$

where $\boldsymbol{\tau} \in \mathbb{R}^{3\times1}$ and $\boldsymbol{A} \in \mathbb{R}^{3\times3}$ denote the translation and orientation between global and body-fixed (floating) coordinate system, respectively, and $\boldsymbol{\theta} \in \mathbb{R}^{n_{\mathrm{r}}\times1}$ denotes a proper rotational parametrization with n_{r} rotational generalized coordinates, e.g., Euler parameters. The flexible deformation of a material point relative to the floating frame $\overline{\boldsymbol{c}}_{\mathrm{f}} \in \mathbb{R}^{3\times1}$ is then conventionally approximated by a Ritz approach as

$$\overline{\boldsymbol{c}}_{\mathrm{f}}(\overline{\boldsymbol{x}},t) = \overline{\boldsymbol{\mathcal{S}}}(\overline{\boldsymbol{x}})\,\overline{\boldsymbol{c}}_{\mathrm{f}}(t), \tag{2}$$

where $\overline{\boldsymbol{\mathcal{S}}} \in \mathbb{R}^{3\times3n_{\mathrm{n}}}$ denotes the finite element shape function matrix and $\overline{\boldsymbol{c}}_{\mathrm{f}} \in \mathbb{R}^{3n_{\mathrm{n}}\times1}$ the (discrete) flexible nodal displacements. Note that in three-dimensional space a displacement-based finite element model with n_{n} nodes has $3n_{\mathrm{n}}$ generalized coordinates and the nodal-displacements are conventionally arranged in the following manner:

$$\overline{\boldsymbol{c}}_{\mathrm{f}} = \begin{bmatrix} \overline{\boldsymbol{c}}_{\mathrm{f}}^{(1)} \\ \vdots \\ \overline{\boldsymbol{c}}_{\mathrm{f}}^{(n_{\mathrm{n}})} \end{bmatrix} \in \mathbb{R}^{3n_{\mathrm{n}}\times1}. \tag{3}$$

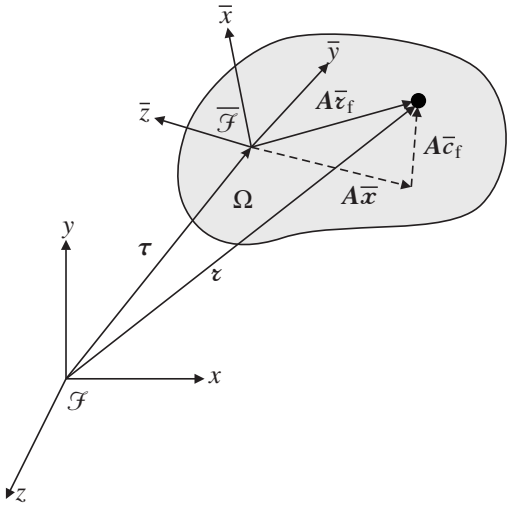

Fig. 1: Continuous body Ω with global $\mathcal{F}$ and floating $\overline{\mathcal{F}}$ frame; the translation between the frames is given by $\boldsymbol{\tau}$ and the orientations are related by the rotation matrix $\boldsymbol{A}$. The position vector $\boldsymbol{r}$ defines the current (continuous) position of a material point $\overline{\boldsymbol{x}}$. The deformation and deformed position of a material point relative to the floating frame are given by $\overline{\boldsymbol{c}}_{\mathrm{f}}$ and $\overline{\boldsymbol{r}}_{\mathrm{f}}$, respectively. Adapted from [102].

The equations of motion are then obtained via, e.g., Lagrange's equation[5], i.e.,

$$\underbrace{\frac{\mathrm{d}}{\mathrm{d}t}\left(\frac{\partial \mathcal{T}}{\partial \dot{\boldsymbol{q}}^{\mathrm{T}}}\right) - \frac{\partial \mathcal{T}}{\partial \boldsymbol{q}^{\mathrm{T}}}}_{\text{inertia forces}} + \underbrace{\frac{\partial \mathcal{U}}{\partial \boldsymbol{q}^{\mathrm{T}}}}_{\text{elastic forces}} + \underbrace{\frac{\partial \boldsymbol{\lambda}^{\mathrm{T}}\boldsymbol{g}}{\partial \boldsymbol{q}^{\mathrm{T}}}}_{\text{constraint forces}} = \underbrace{\frac{\partial \boldsymbol{r}}{\partial \boldsymbol{q}^{\mathrm{T}}}\boldsymbol{f}}_{\text{applied forces}}, \tag{4}$$

[4] Please note that overlined quantities are given with respect to the body-fixed frame in contrast to global quantities, and calligraphic letters denote space-continuous quantities depending on the continuous position of a material point in contrast to discrete quantities.

[5] Any other equivalent method such as the principle of virtual work/power or Hamilton's principle is equally suitable.

with time t, the FFRF generalized coordinates

$$\boldsymbol{q} = \begin{bmatrix} \boldsymbol{\tau} \\ \boldsymbol{\theta} \\ \overline{\boldsymbol{c}}_\mathrm{f} \end{bmatrix}, \tag{5}$$

the n_c Lagrange multipliers $\boldsymbol{\lambda} \in \mathbb{R}^{n_\mathrm{c}\times 1}$, the constraint equations $\boldsymbol{g} = \boldsymbol{0}_{n_\mathrm{c}\times 1}$, and the the applied force vector $\boldsymbol{f} \in \mathbb{R}^{3\times 1}$. The conventional continuum-mechanics-based definitions of the continuous kinetic energy $\mathcal{T}$ and potential energy $\mathcal{U}$ read

$$\mathcal{T} = \frac{1}{2}\int_\mathcal{V} \rho\, \dot{\boldsymbol{r}}^\mathrm{T}\dot{\boldsymbol{r}}\,\mathrm{d}\mathcal{V}, \tag{6}$$

$$\mathcal{U} = \frac{1}{2}\int_\mathcal{V} \overline{\boldsymbol{e}}^\mathrm{T}\overline{\boldsymbol{\sigma}}\,\mathrm{d}\mathcal{V}, \tag{7}$$

with ρ and $\mathcal{V}$ denoting the density and volume of a system body, respectively, and $\overline{\boldsymbol{e}}$ and $\overline{\boldsymbol{\sigma}}$ the (small) strain and stress vector in Voigt notation. This space-continuous definition, especially of the kinetic energy, is a source of trouble in the conventional literature concerning the FFRF, because of the appearance of so-called inertia shape integrals. This may be highlighted with the following equation:

$$\frac{\mathrm{d}}{\mathrm{d}t}\left(\frac{\partial \mathcal{T}}{\partial \dot{\boldsymbol{q}}^\mathrm{T}}\right) - \frac{\partial \mathcal{T}}{\partial \boldsymbol{q}^\mathrm{T}} = \widehat{\boldsymbol{M}}\ddot{\boldsymbol{q}} + \underbrace{\dot{\widehat{\boldsymbol{M}}}\dot{\boldsymbol{q}} - \frac{1}{2}\frac{\partial \dot{\boldsymbol{q}}^\mathrm{T}\widehat{\boldsymbol{M}}\dot{\boldsymbol{q}}}{\partial \boldsymbol{q}^\mathrm{T}}}_{-\widehat{\mathcal{Q}}_\mathrm{v}} \tag{8}$$

$$= \int_\mathcal{V} \bigstar\,\mathrm{d}\mathcal{V}, \tag{9}$$

where $\widehat{\boldsymbol{M}}$ denotes the conventional FFRF mass matrix, $\widehat{\mathcal{Q}}_\mathrm{v}$ the conventional FFRF quadratic velocity vector, and $\bigstar$ is just a placeholder for formulation-specific quantities. It shall be highlighted, that the inertia shape integrals

$$\int_\mathcal{V} \bigstar\,\mathrm{d}\mathcal{V}$$

depend not only on the FFRF generalized coordinates, but also on the finite element shape functions and continuous positions of the material points, which makes the conventional formulation dependent on the algorithmic level of an underlying finite element code. Moreover, this straight forward application of Lagrange's equation (8) involves tedious derivations to obtain the quadratic velocity vector, which may be seen in [78, 103, 76, 77], where entire articles are devoted to the derivation of $\widehat{\mathcal{Q}}_\mathrm{v}$.

Recent developments [90, 102, 104] preclude these hurdles unnecessary. This so-called nodal-based framework will be discussed in Sect. 2.3, but we can already take one idea from [102], i.e., the abstract definition and derivation of the inertia forces, to avoid these aforementioned tedious derivations even without the nodal-based approach. To this end we first differentiate Eq. (1) with respect to time to obtain

$$\dot{\boldsymbol{r}} = \boldsymbol{\mathcal{L}}(\boldsymbol{q})\dot{\boldsymbol{q}}, \tag{10}$$

with

$$\boldsymbol{\mathcal{L}} = \begin{bmatrix} \boldsymbol{I} & -\boldsymbol{A}\widetilde{\overline{\boldsymbol{r}}}_\mathrm{f}\overline{\boldsymbol{G}} & \boldsymbol{A}\overline{\boldsymbol{\mathcal{S}}} \end{bmatrix}, \tag{11}$$

where[6] $\boldsymbol{I} \in \mathbb{R}^{3\times 3}$ denotes the identity matrix. Further quantities in the equation above are

$$\widetilde{\overline{\boldsymbol{r}}}_\mathrm{f} = \widetilde{\overline{\boldsymbol{x}}} + \widetilde{\overline{\boldsymbol{c}}}_\mathrm{f} \tag{12}$$

and the matrix $\overline{\boldsymbol{G}} \in \mathbb{R}^{3\times n_\mathrm{r}}$, which is implicitly defined by the local angular velocity $\overline{\boldsymbol{\omega}} \in \mathbb{R}^{3\times 1}$ and the rotational parametrization as[7]

$$\overline{\boldsymbol{\omega}} = \overline{\boldsymbol{G}}\dot{\boldsymbol{\theta}}. \tag{13}$$

[6] Note that identity and zero matrices are usually displayed with the matrix size as a subscript, e.g., $\boldsymbol{I}_{3\times 3}$, with the only exception of $\boldsymbol{I}$ due to its frequent use, i.e., $\boldsymbol{I}_{3\times 3} = \boldsymbol{I}$.

[7] Note that the generic relationship in Eq. (13) is valid for any set of rotation parameter [31], which means that the presented derivations and equations are valid for any rotation parametrization.

Note that the tilde operator[8] converts any $\mathbb{R}^{3\times1}$ vector in its corresponding skew-symmetric $\mathbb{R}^{3\times3}$ matrix. Furthermore, the identity [76]

$$\frac{\partial \boldsymbol{A}\overline{\boldsymbol{v}}}{\partial \boldsymbol{\theta}} = -\boldsymbol{A}\widetilde{\overline{\boldsymbol{v}}}\,\overline{\boldsymbol{G}}, \tag{15}$$

which is valid for any vector not explicitly depending on $\boldsymbol{\theta}$, has been used to obtain Eq. (11).

The next step is to realize that

$$\mathcal{T} = \mathcal{T}\left(\dot{\boldsymbol{\tau}}\left(\dot{\boldsymbol{q}}, \boldsymbol{q}\right)\right), \tag{16}$$

which enables us to employ the chain and product rule of differentiation elegantly, in line with the nodal-based version presented in [102] – see also Sect. 2.3.2 and Sect. 2.3.3, to obtain

$$\left(\int_{\mathcal{V}} \rho \boldsymbol{\mathcal{L}}^{\mathrm{T}} \boldsymbol{\mathcal{L}} \mathrm{d}\mathcal{V}\right)\ddot{\boldsymbol{q}} + \left(\int_{\mathcal{V}} \rho \boldsymbol{\mathcal{L}}^{\mathrm{T}} \dot{\boldsymbol{\mathcal{L}}} \mathrm{d}\mathcal{V}\right)\dot{\boldsymbol{q}} + \operatorname{diag}\left(\boldsymbol{0}_{3\times3}, \boldsymbol{0}_{n_{\mathrm{r}}\times n_{\mathrm{r}}}, \int_{\mathcal{V}} \overline{\mathcal{D}}^{\mathrm{T}} \overline{\boldsymbol{E}}\, \overline{\mathcal{D}} \mathrm{d}\mathcal{V}\right)\boldsymbol{q} + \mathcal{J}^{\mathrm{T}}\boldsymbol{\lambda} = \boldsymbol{\mathcal{L}}^{\mathrm{T}}\boldsymbol{f}, \tag{17}$$

with

$$\dot{\boldsymbol{\mathcal{L}}} = \begin{bmatrix} \boldsymbol{0}_{n_{\mathrm{r}}\times n_{\mathrm{r}}} & -\boldsymbol{A}\left(\widetilde{\widetilde{\overline{\boldsymbol{\omega}}}\,\overline{\boldsymbol{\tau}}_{\mathrm{f}}}\,\overline{\boldsymbol{G}} + \dot{\widetilde{\overline{\boldsymbol{u}}}}_{\mathrm{f}}\overline{\boldsymbol{G}} + \widetilde{\overline{\boldsymbol{\tau}}}_{\mathrm{f}}\dot{\overline{\boldsymbol{G}}}\right) & \boldsymbol{A}\widetilde{\overline{\boldsymbol{\omega}}}\,\overline{\mathcal{S}} \end{bmatrix}, \tag{18}$$

where the FFRF stiffness matrix includes the matrix of shape function derivatives $\overline{\mathcal{D}}$ and the linearly-elastic material matrix in Voigt notation $\overline{\boldsymbol{E}}$.[9]

Performing the matrix multiplications in Eq. (17) to obtain a more explicit form of the equations of motion yields the conventional (inertia-shape-integral) FFRF, i.e., slightly rearranged

$$\begin{aligned}
&\begin{bmatrix} \int_{\mathcal{V}} \rho \boldsymbol{I} \mathrm{d}\mathcal{V} & -\int_{\mathcal{V}} \rho \boldsymbol{A}\widetilde{\overline{\boldsymbol{\tau}}}_{\mathrm{f}}\overline{\boldsymbol{G}} \mathrm{d}\mathcal{V} & \int_{\mathcal{V}} \rho \boldsymbol{A}\overline{\mathcal{S}} \mathrm{d}\mathcal{V} \\ & \int_{\mathcal{V}} \rho \overline{\boldsymbol{G}}^{\mathrm{T}}\widetilde{\overline{\boldsymbol{\tau}}}_{\mathrm{f}}^{\mathrm{T}}\widetilde{\overline{\boldsymbol{\tau}}}_{\mathrm{f}}\overline{\boldsymbol{G}} \mathrm{d}\mathcal{V} & -\int_{\mathcal{V}} \rho \overline{\boldsymbol{G}}^{\mathrm{T}}\widetilde{\overline{\boldsymbol{\tau}}}_{\mathrm{f}}^{\mathrm{T}}\overline{\mathcal{S}} \mathrm{d}\mathcal{V} \\ \text{sym.} & & \int_{\mathcal{V}} \rho \overline{\mathcal{S}}^{\mathrm{T}}\overline{\mathcal{S}} \mathrm{d}\mathcal{V} \end{bmatrix}\begin{bmatrix} \ddot{\boldsymbol{\tau}} \\ \ddot{\boldsymbol{\theta}} \\ \ddot{\overline{\boldsymbol{c}}}_{\mathrm{f}} \end{bmatrix} = -\begin{bmatrix} \boldsymbol{0}_{3\times3} & & \\ & \boldsymbol{0}_{n_{\mathrm{r}}\times n_{\mathrm{r}}} & \\ & & \int_{\mathcal{V}} \overline{\mathcal{D}}^{\mathrm{T}}\overline{\boldsymbol{E}}\,\overline{\mathcal{D}} \mathrm{d}\mathcal{V} \end{bmatrix}\begin{bmatrix} \boldsymbol{\tau} \\ \boldsymbol{\theta} \\ \overline{\boldsymbol{c}}_{\mathrm{f}} \end{bmatrix} \\
&+ \begin{bmatrix} -\int_{\mathcal{V}} \rho \boldsymbol{A}\left(\widetilde{\overline{\boldsymbol{\omega}}}\,\widetilde{\overline{\boldsymbol{\omega}}}\,\overline{\boldsymbol{\tau}}_{\mathrm{f}} + 2\widetilde{\overline{\boldsymbol{\omega}}}\,\dot{\overline{\boldsymbol{u}}}_{\mathrm{f}} - \dot{\widetilde{\overline{\boldsymbol{\tau}}}}_{\mathrm{f}}\overline{\boldsymbol{G}}\dot{\boldsymbol{\theta}}\right)\mathrm{d}\mathcal{V} \\ \int_{\mathcal{V}} \rho \overline{\boldsymbol{G}}^{\mathrm{T}}\widetilde{\overline{\boldsymbol{\tau}}}_{\mathrm{f}}^{\mathrm{T}}\left(\widetilde{\overline{\boldsymbol{\omega}}}\,\widetilde{\overline{\boldsymbol{\omega}}}\,\overline{\boldsymbol{\tau}}_{\mathrm{f}} + 2\widetilde{\overline{\boldsymbol{\omega}}}\,\dot{\overline{\boldsymbol{u}}}_{\mathrm{f}} - \dot{\widetilde{\overline{\boldsymbol{\tau}}}}_{\mathrm{f}}\overline{\boldsymbol{G}}\dot{\boldsymbol{\theta}}\right)\mathrm{d}\mathcal{V} \\ -\int_{\mathcal{V}} \rho \overline{\mathcal{S}}^{\mathrm{T}}\left(\widetilde{\overline{\boldsymbol{\omega}}}\,\widetilde{\overline{\boldsymbol{\omega}}}\,\overline{\boldsymbol{\tau}}_{\mathrm{f}} + 2\widetilde{\overline{\boldsymbol{\omega}}}\,\dot{\overline{\boldsymbol{u}}}_{\mathrm{f}} - \dot{\widetilde{\overline{\boldsymbol{\tau}}}}_{\mathrm{f}}\overline{\boldsymbol{G}}\dot{\boldsymbol{\theta}}\right)\mathrm{d}\mathcal{V} \end{bmatrix} \\
&+ \begin{bmatrix} \boldsymbol{I} \\ -\overline{\boldsymbol{G}}^{\mathrm{T}}\widetilde{\overline{\boldsymbol{\tau}}}_{\mathrm{f}}^{\mathrm{T}}\boldsymbol{A}^{\mathrm{T}} \\ \overline{\mathcal{S}}^{\mathrm{T}}\boldsymbol{A}^{\mathrm{T}} \end{bmatrix}\boldsymbol{f} - \frac{\partial \boldsymbol{g}}{\partial \boldsymbol{q}^{\mathrm{T}}}\boldsymbol{\lambda},
\end{aligned} \tag{19}$$

where

$$\overline{\boldsymbol{M}} = \int_{\mathcal{V}} \rho \overline{\mathcal{S}}^{\mathrm{T}}\overline{\mathcal{S}} \mathrm{d}\mathcal{V} \tag{20}$$

and

$$\overline{\boldsymbol{K}} = \int_{\mathcal{V}} \overline{\mathcal{D}}^{\mathrm{T}}\overline{\boldsymbol{E}}\,\overline{\mathcal{D}} \mathrm{d}\mathcal{V} \tag{21}$$

are the constant mass and stiffness matrices known from linear elastodynamics, respectively.

[8]
$$\boldsymbol{v} = \begin{bmatrix} v_1 \\ v_2 \\ v_3 \end{bmatrix} \quad \Rightarrow \quad \widetilde{\boldsymbol{v}} = \begin{bmatrix} 0 & -v_3 & v_2 \\ v_3 & 0 & -v_1 \\ -v_2 & v_1 & 0 \end{bmatrix} \tag{14}$$

[9] Note that $\overline{\boldsymbol{e}} = \overline{\mathcal{D}}\,\overline{\boldsymbol{c}}_{\mathrm{f}}$ and $\overline{\boldsymbol{s}} = \overline{\boldsymbol{E}}\,\overline{\boldsymbol{e}}$ are the standard expressions from the linear finite element method, see, e.g., [105].

2.2.2 Component mode synthesis floating frame of reference formulation

Within the CMS the flexible deformation is approximated by[10]

$$\overline{\boldsymbol{c}}_{\mathrm{f}} \approx \overline{\boldsymbol{\Psi}}\boldsymbol{\zeta} \quad \text{with} \quad n_{\mathrm{m}} = \dim(\boldsymbol{\zeta}) \ll \dim(\overline{\boldsymbol{c}}_{\mathrm{f}}) = 3n_{\mathrm{n}}, \tag{22}$$

where $\overline{\boldsymbol{\Psi}} \in \mathbb{R}^{3n_{\mathrm{n}} \times n_{\mathrm{m}}}$ contains column-wise the modes included in the reduction basis, i.e., a low-dimensional solution subspace, and $\boldsymbol{\zeta} \in \mathbb{R}^{n_{\mathrm{m}} \times 1}$ are the associated modal coordinates. Therefore, the reduction for all generalized coordinates follows as

$$\begin{bmatrix} \boldsymbol{\tau} \\ \boldsymbol{\theta} \\ \overline{\boldsymbol{c}}_{\mathrm{f}} \end{bmatrix} \approx \begin{bmatrix} \boldsymbol{I} & & \\ & \boldsymbol{I}_{n_{\mathrm{r}} \times n_{\mathrm{r}}} & \\ & & \overline{\boldsymbol{\Psi}} \end{bmatrix} \begin{bmatrix} \boldsymbol{\tau} \\ \boldsymbol{\theta} \\ \boldsymbol{\zeta} \end{bmatrix}, \tag{23}$$

where $\boldsymbol{I}_{n_{\mathrm{r}} \times n_{\mathrm{r}}}$ is an identity matrix of proper size. Substituting Eq. (23) into Eq. (19) and left-multiplying the result with the transposed of $\operatorname{diag}\left(\boldsymbol{I}, \boldsymbol{I}_{n_{\mathrm{r}} \times n_{\mathrm{r}}}, \overline{\boldsymbol{\Psi}}\right)$ yields the nodal-based equations of motion in the reduced space, i.e.,

$$\begin{aligned}
&\begin{bmatrix} \int_{\mathcal{V}} \rho \boldsymbol{I} \mathrm{d}\mathcal{V} & -\int_{\mathcal{V}} \rho \boldsymbol{A} \widetilde{\overline{\boldsymbol{r}}}_{\mathrm{f}} \overline{\boldsymbol{G}} \mathrm{d}\mathcal{V} & \int_{\mathcal{V}} \rho \boldsymbol{A} \overline{\mathcal{S}}\, \overline{\boldsymbol{\Psi}} \mathrm{d}\mathcal{V} \\ & \int_{\mathcal{V}} \rho \overline{\boldsymbol{G}}^{\mathrm{T}} \widetilde{\overline{\boldsymbol{r}}}_{\mathrm{f}}^{\mathrm{T}} \widetilde{\overline{\boldsymbol{r}}}_{\mathrm{f}} \overline{\boldsymbol{G}} \mathrm{d}\mathcal{V} & -\int_{\mathcal{V}} \rho \overline{\boldsymbol{G}}^{\mathrm{T}} \widetilde{\overline{\boldsymbol{r}}}_{\mathrm{f}}^{\mathrm{T}} \overline{\mathcal{S}}\, \overline{\boldsymbol{\Psi}} \mathrm{d}\mathcal{V} \\ \text{sym.} & & \int_{\mathcal{V}} \rho \overline{\boldsymbol{\Psi}}^{\mathrm{T}} \overline{\mathcal{S}}^{\mathrm{T}} \overline{\mathcal{S}}\, \overline{\boldsymbol{\Psi}} \mathrm{d}\mathcal{V} \end{bmatrix} \begin{bmatrix} \ddot{\boldsymbol{\tau}} \\ \ddot{\boldsymbol{\theta}} \\ \ddot{\boldsymbol{\zeta}} \end{bmatrix} = -\begin{bmatrix} \boldsymbol{0}_{3\times 3} & & \\ & \boldsymbol{0}_{n_{\mathrm{r}} \times n_{\mathrm{r}}} & \\ & & \int_{\mathcal{V}} \overline{\boldsymbol{\Psi}}^{\mathrm{T}} \overline{\mathcal{D}}^{\mathrm{T}} \overline{\boldsymbol{E}}\, \overline{\mathcal{D}}\, \overline{\boldsymbol{\Psi}} \mathrm{d}\mathcal{V} \end{bmatrix} \begin{bmatrix} \boldsymbol{\tau} \\ \boldsymbol{\theta} \\ \boldsymbol{\zeta} \end{bmatrix} \\
&+ \begin{bmatrix} -\int_{\mathcal{V}} \rho \boldsymbol{A} \left(\widetilde{\overline{\boldsymbol{\omega}}}\, \widetilde{\overline{\boldsymbol{\omega}}}\, \overline{\boldsymbol{r}}_{\mathrm{f}} + 2\widetilde{\overline{\boldsymbol{\omega}}}\, \dot{\overline{\boldsymbol{u}}}_{\mathrm{f}} - \widetilde{\overline{\boldsymbol{r}}}_{\mathrm{f}} \overline{\boldsymbol{G}} \dot{\boldsymbol{\theta}} \right) \mathrm{d}\mathcal{V} \\ \int_{\mathcal{V}} \rho \overline{\boldsymbol{G}}^{\mathrm{T}} \widetilde{\overline{\boldsymbol{r}}}_{\mathrm{f}}^{\mathrm{T}} \left(\widetilde{\overline{\boldsymbol{\omega}}}\, \widetilde{\overline{\boldsymbol{\omega}}}\, \overline{\boldsymbol{r}}_{\mathrm{f}} + 2\widetilde{\overline{\boldsymbol{\omega}}}\, \dot{\overline{\boldsymbol{u}}}_{\mathrm{f}} - \widetilde{\overline{\boldsymbol{r}}}_{\mathrm{f}} \overline{\boldsymbol{G}} \dot{\boldsymbol{\theta}} \right) \mathrm{d}\mathcal{V} \\ -\int_{\mathcal{V}} \rho \overline{\boldsymbol{\Psi}}^{\mathrm{T}} \overline{\mathcal{S}}^{\mathrm{T}} \left(\widetilde{\overline{\boldsymbol{\omega}}}\, \widetilde{\overline{\boldsymbol{\omega}}}\, \overline{\boldsymbol{r}}_{\mathrm{f}} + 2\widetilde{\overline{\boldsymbol{\omega}}}\, \dot{\overline{\boldsymbol{u}}}_{\mathrm{f}} - \widetilde{\overline{\boldsymbol{r}}}_{\mathrm{f}} \overline{\boldsymbol{G}} \dot{\boldsymbol{\theta}} \right) \mathrm{d}\mathcal{V} \end{bmatrix} \\
&+ \begin{bmatrix} \boldsymbol{I} \\ -\overline{\boldsymbol{G}}^{\mathrm{T}} \widetilde{\overline{\boldsymbol{r}}}_{\mathrm{f}}^{\mathrm{T}} \\ \overline{\boldsymbol{\Psi}}^{\mathrm{T}} \overline{\mathcal{S}}^{\mathrm{T}} \end{bmatrix} \boldsymbol{A}^{\mathrm{T}} \boldsymbol{f} - \frac{\partial \boldsymbol{g}}{\partial \boldsymbol{q}^{\mathrm{T}}} \boldsymbol{\lambda}.
\end{aligned} \tag{24}$$

2.2.3 Lumped-mass floating frame of reference formulation

To circumvent the evaluation of the inertia shape integrals of the conventional FFRF, commercial flexible multibody packages like ADAMS or RecurDyn resort, and are strictly limited, to a lumped mass approach according to [31], see, e.g., [72, 71].

Within the approximate lumped mass approach a so-called nodal mass $m^{(i)}$ for translational generalized coordinates or a nodal inertia for rotational generalized coordinates is assigned to each finite element nodal generalized coordinate. If the finite element nodes have only translational generalized coordinates, the kinetic energy of each flexible body is in turn approximately calculated by the sum of all nodal generalized coordinate contributions according to particle dynamics theory, i.e., [31, 72]

$$\mathcal{T} \approx \frac{1}{2} \sum_{i=1}^{n_{\mathrm{n}}} m^{(i)} \left(\dot{\overline{\boldsymbol{r}}}^{(i)} \right)^{\mathrm{T}} \dot{\overline{\boldsymbol{r}}}^{(i)}, \tag{25}$$

where

$$\dot{\overline{\boldsymbol{r}}}^{(i)} = \boldsymbol{L}^{(i)} \dot{\boldsymbol{q}} \tag{26}$$

with

$$\boldsymbol{L}^{(i)} = \begin{bmatrix} \boldsymbol{I} & -\widetilde{\overline{\boldsymbol{r}}}_{\mathrm{f}}^{(i)} \overline{\boldsymbol{G}} & \boldsymbol{A}\boldsymbol{B}^{(i)} \end{bmatrix} \tag{27}$$

and $\boldsymbol{B}^{(i)} = \begin{bmatrix} \boldsymbol{0}_{3\times 3} & \dots & \boldsymbol{0}_{3\times 3} & \boldsymbol{I} & \boldsymbol{0}_{3\times 3} & \dots & \boldsymbol{0}_{3\times 3} \end{bmatrix}$ is just a Boolean matrix extracting the nodal quantities of node (i) from the overall nodal quantities, i.e.,

$$\dot{\overline{\boldsymbol{c}}}_{\mathrm{f}}^{(i)} = \boldsymbol{B}^{(i)} \dot{\overline{\boldsymbol{c}}}_{\mathrm{f}}. \tag{28}$$

[10] The equality sign is used in the following equations for the sake of simplicity even though the CMS introduces an approximation if $\dim(\boldsymbol{\zeta}) < \dim(\overline{\boldsymbol{c}}_{\mathrm{f}})$.

Hence, all inertia shape integrals in Eq. (17) are replaced and approximated by sums, i.e.,

$$\widehat{m} \approx \widehat{M}^{\text{lumped}} = \sum_{i=1}^{n_\text{n}} m^{(i)} \left(\boldsymbol{L}^{(i)}\right)^\text{T} \boldsymbol{L}^{(i)} \tag{29}$$

$$= \sum_{i=1}^{n_\text{n}} m^{(i)} \begin{bmatrix} \boldsymbol{I} & -\boldsymbol{A}\widetilde{\overline{\boldsymbol{r}}}_\text{f}^{(i)}\overline{\boldsymbol{G}} & \boldsymbol{A}\overline{\boldsymbol{B}}^{(i)} \\ & \overline{\boldsymbol{G}}^\text{T}\left(\widetilde{\overline{\boldsymbol{r}}}_\text{f}^{(i)}\right)^\text{T}\widetilde{\overline{\boldsymbol{r}}}_\text{f}^{(i)}\overline{\boldsymbol{G}} & -\overline{\boldsymbol{G}}^\text{T}\left(\widetilde{\overline{\boldsymbol{r}}}_\text{f}^{(i)}\right)^\text{T}\overline{\boldsymbol{B}}^{(i)} \\ \text{sym.} & & \left(\overline{\boldsymbol{B}}^{(i)}\right)^\text{T}\overline{\boldsymbol{B}}^{(i)} \end{bmatrix}, \tag{30}$$

$$\widehat{\mathcal{Q}}_\text{v} \approx \widehat{\boldsymbol{Q}}_\text{v}^{\text{lumped}} = -\sum_{i=1}^{n_\text{n}} m^{(i)} \left(\boldsymbol{L}^{(i)}\right)^\text{T} \dot{\boldsymbol{L}}^{(i)}\dot{\boldsymbol{q}} \tag{31}$$

$$= \sum_{i=1}^{n_\text{n}} m^{(i)} \begin{bmatrix} -\boldsymbol{A}\left(\widetilde{\overline{\boldsymbol{\omega}}}\,\widetilde{\overline{\boldsymbol{\omega}}}\,\overline{\boldsymbol{r}}_\text{f}^{(i)} + 2\widetilde{\overline{\boldsymbol{\omega}}}\,\dot{\overline{\boldsymbol{c}}}_\text{f}^{(i)} - \widetilde{\overline{\boldsymbol{r}}}_\text{f}^{(i)}\dot{\overline{\boldsymbol{G}}}\dot{\boldsymbol{\theta}}\right) \\ \overline{\boldsymbol{G}}^\text{T}\left(\widetilde{\overline{\boldsymbol{r}}}_\text{f}^{(i)}\right)^\text{T}\left(\widetilde{\overline{\boldsymbol{\omega}}}\,\widetilde{\overline{\boldsymbol{\omega}}}\,\overline{\boldsymbol{r}}_\text{f}^{(i)} + 2\widetilde{\overline{\boldsymbol{\omega}}}\,\dot{\overline{\boldsymbol{c}}}_\text{f}^{(i)} - \widetilde{\overline{\boldsymbol{r}}}_\text{f}^{(i)}\dot{\overline{\boldsymbol{G}}}\dot{\boldsymbol{\theta}}\right) \\ -\left(\overline{\boldsymbol{B}}^{(i)}\right)^\text{T}\left(\widetilde{\overline{\boldsymbol{\omega}}}\,\widetilde{\overline{\boldsymbol{\omega}}}\,\overline{\boldsymbol{r}}_\text{f}^{(i)} + 2\widetilde{\overline{\boldsymbol{\omega}}}\,\dot{\overline{\boldsymbol{c}}}_\text{f}^{(i)} - \widetilde{\overline{\boldsymbol{r}}}_\text{f}^{(i)}\dot{\overline{\boldsymbol{G}}}\dot{\boldsymbol{\theta}}\right) \end{bmatrix}, \tag{32}$$

or with modal reduction

$$\widehat{\boldsymbol{M}}^{\text{lumped}} \approx \sum_{i=1}^{n_\text{n}} m^{(i)} \begin{bmatrix} \boldsymbol{I} & -\boldsymbol{A}\widetilde{\overline{\boldsymbol{r}}}_\text{f}^{(i)}\overline{\boldsymbol{G}} & \boldsymbol{A}\overline{\boldsymbol{B}}^{(i)}\overline{\boldsymbol{\Psi}} \\ & \overline{\boldsymbol{G}}^\text{T}\left(\widetilde{\overline{\boldsymbol{r}}}_\text{f}^{(i)}\right)^\text{T}\widetilde{\overline{\boldsymbol{r}}}_\text{f}^{(i)}\overline{\boldsymbol{G}} & -\overline{\boldsymbol{G}}^\text{T}\left(\widetilde{\overline{\boldsymbol{r}}}_\text{f}^{(i)}\right)^\text{T}\overline{\boldsymbol{B}}^{(i)}\overline{\boldsymbol{\Psi}} \\ \text{sym.} & & \overline{\boldsymbol{\Psi}}^\text{T}\left(\overline{\boldsymbol{B}}^{(i)}\right)^\text{T}\overline{\boldsymbol{B}}^{(i)}\overline{\boldsymbol{\Psi}} \end{bmatrix}, \tag{33}$$

$$\widehat{\boldsymbol{Q}}_\text{v}^{\text{lumped}} \approx \sum_{i=1}^{n_\text{n}} m^{(i)} \begin{bmatrix} -\boldsymbol{A}\left(\widetilde{\overline{\boldsymbol{\omega}}}\,\widetilde{\overline{\boldsymbol{\omega}}}\,\overline{\boldsymbol{r}}_\text{f}^{(i)} + 2\widetilde{\overline{\boldsymbol{\omega}}}\,\dot{\overline{\boldsymbol{c}}}_\text{f}^{(i)} - \widetilde{\overline{\boldsymbol{r}}}_\text{f}^{(i)}\dot{\overline{\boldsymbol{G}}}\dot{\boldsymbol{\theta}}\right) \\ \overline{\boldsymbol{G}}^\text{T}\left(\widetilde{\overline{\boldsymbol{r}}}_\text{f}^{(i)}\right)^\text{T}\left(\widetilde{\overline{\boldsymbol{\omega}}}\,\widetilde{\overline{\boldsymbol{\omega}}}\,\overline{\boldsymbol{r}}_\text{f}^{(i)} + 2\widetilde{\overline{\boldsymbol{\omega}}}\,\dot{\overline{\boldsymbol{c}}}_\text{f}^{(i)} - \widetilde{\overline{\boldsymbol{r}}}_\text{f}^{(i)}\dot{\overline{\boldsymbol{G}}}\dot{\boldsymbol{\theta}}\right) \\ -\overline{\boldsymbol{\Psi}}^\text{T}\left(\overline{\boldsymbol{B}}^{(i)}\right)^\text{T}\left(\widetilde{\overline{\boldsymbol{\omega}}}\,\widetilde{\overline{\boldsymbol{\omega}}}\,\overline{\boldsymbol{r}}_\text{f}^{(i)} + 2\widetilde{\overline{\boldsymbol{\omega}}}\,\dot{\overline{\boldsymbol{c}}}_\text{f}^{(i)} - \widetilde{\overline{\boldsymbol{r}}}_\text{f}^{(i)}\dot{\overline{\boldsymbol{G}}}\dot{\boldsymbol{\theta}}\right) \end{bmatrix}. \tag{34}$$

This is a significant simplification, but enables commercial multibody software packages to calculate the so-called FFRF invariants, which are constant "ingredients" required to set up the FFRF mass matrix and quadratic velocity vector – approximately.[11] These invariants may be found in the documentations of commercial multibody software packages, see, e.g., RecurDyn [71] and Adams [72]. It shall be highlighted that the lumped mass invariants employed by commercial codes may be obtained by employing a lumped finite element mass matrix in the calculation of the consistent nodal-based invariants presented in Sect. 2.3.4.

Despite the above mentioned inconveniences, the continuum mechanics derivation of the FFRF equations of motion has become a standard in the multibody dynamics literature [31], and also recent papers follow the continuum mechanics approach [103, 76, 77, 78, 79].

The unification framework presented in the following sections of this paper eliminate the aforementioned drawbacks, and excels due to the following properties:

- It eliminates the necessity for a lumped mass approximation.
- It enables simple and concise derivations of linearly-elastic flexible multibody formulations.
- It establishes the formal relationship between linearly-elastic flexible multibody formulations, and highlights the fact that the formulations differ only in the choice of the generalized coordinates.

[11] Note that a consistent mass matrix may not give the best results [106], e.g., a combination of consistent and lumped mass matrix can provide better solutions [107, 106] depending on the application. Furthermore, a lumped mass formulation suffers no loss in the order of convergence in the solution of second order equations employing simple interpolation functions, but is inferior compared to a consistent mass formulation in terms of convergence rate in the solution of higher order equations / second order equations employing more accurate interpolation functions [108].

2.3 A common, nodal-based framework to derive the equations of motion of linearly-elastic flexible multibody systems

2.3.1 Kinematics of flexible bodies subjected to large rigid body motion

As already mentioned, multibody dynamicists often resort to a decomposition of the overall motion into rigid body translation, rigid body rotation, and flexible deformation. This decomposition plays an important role in all the hereinafter presented linearly-elastic flexible multibody formulations.

To understand this common underlying kinematic description, we resort to Fig. 2. Let, again, $\mathcal{I}$ be a global coordinate system, fixed in space and time, and $\overline{\mathcal{I}}$ a floating frame attached to a representative flexible body Ω. The translation and the orientation between the two coordinate systems is again described by the position vector $\boldsymbol{\tau}$ and the rotation matrix $\boldsymbol{A}$.

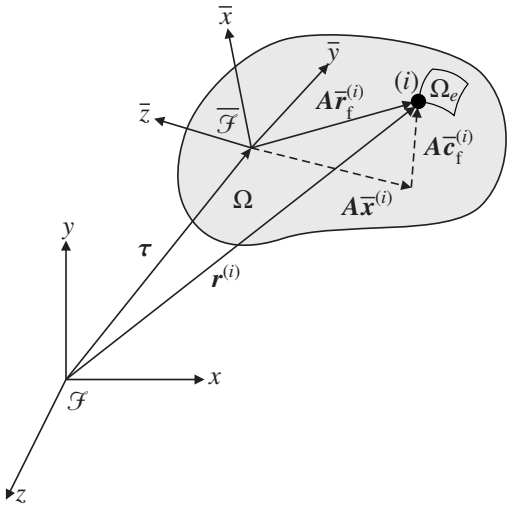

Fig. 2: Finite element discretized body Ω with global $\mathcal{I}$ and floating $\overline{\mathcal{I}}$ frame; the translation between the frames is given by $\boldsymbol{\tau}$ and the orientations are related by the rotation matrix $\boldsymbol{A}$. The position vector $\boldsymbol{r}^{(i)}$ defines the current position of node (i). The flexible nodal displacement and deformed nodal position of node (i) relative to the floating frame are given by $\overline{\boldsymbol{c}}_{\mathrm{f}}^{(i)}$ and $\overline{\boldsymbol{r}}_{\mathrm{f}}^{(i)}$, respectively. Furthermore, Ω_e depicts a representative element of the finite element mesh. Adapted from [102].

The body Ω is discretized with solid (continuum) finite elements Ω_e yielding n_{n} nodes in total. The fundamental decomposition of the displacement in its translational, rotational and flexible part, is also employed within the present framework, but on a nodal-based level. This means we treat each flexible body in its spatially discretized state ab initio, wherefore, only a finite number of points – the finite element nodes – may be in motion. Therefore, the global and overall current nodal position is given by the reference position $\boldsymbol{x}_{\mathrm{ref}}^{(i)} \in \mathbb{R}^{3\times1}$ plus the nodal displacement $\boldsymbol{c}^{(i)} \in \mathbb{R}^{3\times1}$ of node (i) which is decomposed into its translational $\boldsymbol{c}_{\mathrm{t}}^{(i)} \in \mathbb{R}^{3\times1}$, its rotational $\boldsymbol{c}_{\mathrm{r}}^{(i)} \in \mathbb{R}^{3\times1}$, and its flexible part $\boldsymbol{c}_{\mathrm{f}}^{(i)} \in \mathbb{R}^{3\times1}$. Hence, the global position of each node is given by (Fig. 2)

$$\boldsymbol{r}^{(i)} = \boldsymbol{x}_{\mathrm{ref}}^{(i)} + \boldsymbol{c}^{(i)} \tag{35}$$

with

$$\boldsymbol{c}^{(i)} = \boldsymbol{c}_{\mathrm{t}}^{(i)} + \boldsymbol{c}_{\mathrm{r}}^{(i)} + \boldsymbol{c}_{\mathrm{f}}^{(i)}. \tag{36}$$

All finite element nodes of the body share the same displacement for a rigid body translation, i.e. – assuming without loss of generality that the coordinate systems $\mathcal{I}$ and $\overline{\mathcal{I}}$ coincide in the reference configuration[12] – the translation $\boldsymbol{\tau}$ between global $\mathcal{I}$ and local $\overline{\mathcal{I}}$ frame (Fig. 2), hence,

$$\boldsymbol{c}_{\mathrm{t}}^{(i)} = \boldsymbol{\tau}. \tag{38}$$

[12] In other words (Fig. 2)

$$\boldsymbol{\tau}_{\mathrm{ref}} = \boldsymbol{0}_{3\times1} \quad \text{and} \quad \boldsymbol{A}_{\mathrm{ref}} = \boldsymbol{I} \quad \Rightarrow \quad \boldsymbol{x}_{\mathrm{ref}}^{(i)} = \overline{\boldsymbol{x}}^{(i)}. \tag{37}$$

Similarly, the displacement associated with a rigid body rotation of node (i) is given by – again assuming without loss of generality that the coordinate systems $\mathcal{I}$ and $\overline{\mathcal{I}}$ initially coincide[12] – the position of node (i) after rotation $\boldsymbol{A}\overline{\boldsymbol{x}}^{(i)}$ minus its reference position $\overline{\boldsymbol{x}}^{(i)}$, i.e.,

$$\boldsymbol{c}_{\mathrm{r}}^{(i)} = (\boldsymbol{A} - \boldsymbol{I})\,\overline{\boldsymbol{x}}^{(i)}, \tag{39}$$

where $\overline{\boldsymbol{x}}^{(i)} \in \mathbb{R}^{3\times 1}$ denotes the undeformed (reference) nodal coordinates of node (i) expressed in $\overline{\mathcal{I}}$.

Finally, the rotation matrix $\boldsymbol{A}$ may be employed to express a local quantity in the global frame $\mathcal{I}$. Hence, the global flexible nodal displacement of node (i) is given by

$$\boldsymbol{c}_{\mathrm{f}}^{(i)} = \boldsymbol{A}\overline{\boldsymbol{c}}_{\mathrm{f}}^{(i)}, \tag{40}$$

where $\overline{\boldsymbol{c}}_{\mathrm{f}}^{(i)}$ denotes the flexible part of the nodal displacement of node (i) relative to the floating frame $\overline{\mathcal{I}}$, as used in linear finite element analyses.

Combining Eqs. (35) to (40) yields the global overall nodal positions,

$$\boldsymbol{r}^{(i)} = \boldsymbol{\tau} + \boldsymbol{A}\overline{\boldsymbol{x}}^{(i)} + \boldsymbol{A}\overline{\boldsymbol{c}}_{\mathrm{f}}^{(i)}, \tag{41}$$

which may be written in a single block/nodal column matrix for all finite element nodes as [90]

$$\boldsymbol{r} = (\boldsymbol{1}\otimes\boldsymbol{I})\,\boldsymbol{\tau} + \boldsymbol{A}_{\mathrm{bd}}\overline{\boldsymbol{x}} + \boldsymbol{A}_{\mathrm{bd}}\overline{\boldsymbol{c}}_{\mathrm{f}}, \tag{42}$$

where

$$\boldsymbol{1} = \begin{bmatrix} 1 & \dots & 1 \end{bmatrix}^{\mathrm{T}} \in \mathbb{R}^{n_{\mathrm{n}}\times 1} \tag{43}$$

is a single column matrix containing only ones and $\otimes$ denotes Kronecker's product[13] such that $(\boldsymbol{1}\otimes\boldsymbol{I})$ contains the rigid body translation modes and, therefore, simply applies the translation $\boldsymbol{\tau}$ to all finite element nodes, and

$$\boldsymbol{A}_{\mathrm{bd}} = \mathrm{diag}(\boldsymbol{A},\dots,\boldsymbol{A}) \in \mathbb{R}^{3n_{\mathrm{n}}\times 3n_{\mathrm{n}}} \tag{45}$$

denotes an associated block-diagonal matrix with the rotation matrix on its diagonal. Note, again, all herein mentioned block/nodal column matrices, such as $\boldsymbol{r}$, $\overline{\boldsymbol{x}}$, $\overline{\boldsymbol{c}}_{\mathrm{f}}$, $\dots \in \mathbb{R}^{3n_{\mathrm{n}}\times 1}$, are arranged in the standard finite element manner, i.e.,

$$\boldsymbol{r} = \begin{bmatrix} \boldsymbol{r}^{(1)} \\ \vdots \\ \boldsymbol{r}^{(n_{\mathrm{n}})} \end{bmatrix} \in \mathbb{R}^{3n_{\mathrm{n}}\times 1}. \tag{46}$$

Summary of the main result of Sect. 2.3.1 – kinematics of flexible bodies subjected to large rigid body motion

The main result of this section, that will be used throughout this paper, is the kinematic description, stated in Eq. (42), of the positions of all finite element nodes $\boldsymbol{r}$ in terms of the rigid body translation (described by the translation $\boldsymbol{\tau}$ between global and floating frame), the rigid body rotation (described by the rotation matrix $\boldsymbol{A}$ or more precisely the block-diagonal version $\boldsymbol{A}_{\mathrm{bd}}$ of it), and the flexible deformation (described by the flexible nodal displacements of all finite element nodes $\overline{\boldsymbol{c}}_{\mathrm{f}}$), i.e., restated here for presentation purposes,

$$\boldsymbol{r} = (\boldsymbol{1}\otimes\boldsymbol{I})\,\boldsymbol{\tau} + \boldsymbol{A}_{\mathrm{bd}}\,(\overline{\boldsymbol{x}} + \overline{\boldsymbol{c}}_{\mathrm{f}})$$

with the rigid body translation modes $(\boldsymbol{1}\otimes\boldsymbol{I})$ and the constant nodal coordinates of all finite element nodes $\overline{\boldsymbol{x}}$ relative to the floating frame.

[13] If $\boldsymbol{R}\in\mathbb{R}^{m\times n}$ and $\boldsymbol{T}\in\mathbb{R}^{p\times q}$, then $(\boldsymbol{R}\otimes\boldsymbol{T})\in\mathbb{R}^{pm\times qn}$:

$$\boldsymbol{R}\otimes\boldsymbol{T} = \begin{bmatrix} R_{11}\boldsymbol{T} & \cdots & R_{1n}\boldsymbol{T} \\ \vdots & \ddots & \vdots \\ R_{m1}\boldsymbol{T} & \cdots & R_{mn}\boldsymbol{T} \end{bmatrix}. \tag{44}$$

2.3.2 Generic form of the equations of motion

The equations of motion of a spatially-discretized (finite element) mechanical system may be derived via Lagrange's equation, i.e.,

$$\underbrace{\frac{\mathrm{d}}{\mathrm{d}t}\left(\frac{\partial T}{\partial \dot{\boldsymbol{q}}^{\mathrm{T}}}\right) - \frac{\partial T}{\partial \boldsymbol{q}^{\mathrm{T}}}}_{\substack{\text{inertia}\\ \text{forces}}} + \underbrace{\frac{\partial U}{\partial \boldsymbol{q}^{\mathrm{T}}}}_{\substack{\text{elastic}\\ \text{forces}}} + \underbrace{\frac{\partial \boldsymbol{\lambda}^{\mathrm{T}}\boldsymbol{g}}{\partial \boldsymbol{q}^{\mathrm{T}}}}_{\substack{\text{constraint}\\ \text{forces}}} = \underbrace{\frac{\partial \boldsymbol{r}}{\partial \boldsymbol{q}^{\mathrm{T}}}\boldsymbol{f}}_{\substack{\text{applied}\\ \text{forces}}}, \tag{47}$$

where now T denotes the (spatially-discrete) kinetic energy, U denotes the (spatially-discrete) strain energy, $\boldsymbol{g} = \boldsymbol{0}_{n_{\mathrm{c}}\times 1}$ the (spatially-discrete) constraint equations. Furthermore, $\boldsymbol{f} \in \mathbb{R}^{3n_{\mathrm{n}}\times 1}$ contains the applied nodal forces for all finite element nodes, and $\boldsymbol{q} \in \mathbb{R}^{n_q\times 1}$ contains n_q generalized coordinates.

A key aspect to enable the concise and unified nodal-based treatment is to define the system energies on a semi-discrete (nodal-based) level. The nodal-based system energies of linearly-elastic multibody systems may be defined as [90, 102]

$$U = \frac{1}{2}\overline{\boldsymbol{c}}_{\mathrm{f}}^{\mathrm{T}}\,\overline{\boldsymbol{K}}\,\overline{\boldsymbol{c}}_{\mathrm{f}}, \tag{48}$$

$$T = \frac{1}{2}\dot{\boldsymbol{r}}^{\mathrm{T}}\,\overline{\boldsymbol{M}}\,\dot{\boldsymbol{r}}, \tag{49}$$

where $\overline{\boldsymbol{K}} \in \mathbb{R}^{3n_{\mathrm{n}}\times 3n_{\mathrm{n}}}$ denotes the constant finite element stiffness matrix and $\overline{\boldsymbol{M}} \in \mathbb{R}^{3n_{\mathrm{n}}\times 3n_{\mathrm{n}}}$ the constant (consistent) finite element mass matrix from linear elastodynamics. It is important to emphasize the differences in the nodal quantities used to define the system energies. On the one hand, only the flexible part of the nodal displacements contributes to the strain energy, which is attributed to the fact that rigid body displacements cannot give rise to stresses and strains (elastic forces), which is why, Eq. (48) is stated in terms of $\overline{\boldsymbol{c}}_{\mathrm{f}}$. On the other hand, rigid body translations and rotations contribute, of course, to the kinetic energy of the finite element-discretized body, which is why, it is expressed in terms of $\dot{\boldsymbol{r}}$. Furthermore, it is clear that it makes only sense to multiply quantities expressed in the same coordinate system, which is fulfilled here; this is obvious for U , but in fact the consistent finite element mass matrix is assembled with respect to the floating frame $\overline{\mathcal{F}}$ and multiplied with the global nodal velocities expressed in $\mathcal{F}$.

However, there are at least two explanations to justify Eq. (49):

(i) The consistent finite element mass matrix generated with displacement-based finite elements, or in more general terms with identical shape functions $\overline{\mathcal{S}} \in \mathbb{R}^{3\times 3n_{\mathrm{n}}}$ (Eq. (53)) used to interpolate all coordinate directions, such as, using ABAQUS (Dassault Systèmes) terminology, C3D4, C3D8, C3D10, C3D20 elements, is invariant to translations and rotations, i.e., $\boldsymbol{M} = \overline{\boldsymbol{M}}$ and hence

$$\boldsymbol{M} = \boldsymbol{A}_{\mathrm{bd}}^{\mathrm{T}}\boldsymbol{M}\boldsymbol{A}_{\mathrm{bd}} \quad \Leftrightarrow \quad \boldsymbol{M}\boldsymbol{A}_{\mathrm{bd}} = \boldsymbol{A}_{\mathrm{bd}}\boldsymbol{M}, \tag{50}$$

$$\overline{\boldsymbol{M}} = \boldsymbol{A}_{\mathrm{bd}}^{\mathrm{T}}\overline{\boldsymbol{M}}\boldsymbol{A}_{\mathrm{bd}} \quad \Leftrightarrow \quad \overline{\boldsymbol{M}}\boldsymbol{A}_{\mathrm{bd}} = \boldsymbol{A}_{\mathrm{bd}}\overline{\boldsymbol{M}}. \tag{51}$$

In fact any matrix composed out of $\gamma_{ij}\boldsymbol{I}$-blocks, where γ_{ij} are scalars, i.e.,

$$\boldsymbol{\Gamma} = \begin{bmatrix} \gamma_{11}\boldsymbol{I} & \dots & \gamma_{1n}\boldsymbol{I} \\ \vdots & \ddots & \vdots \\ \gamma_{n1}\boldsymbol{I} & \dots & \gamma_{nn}\boldsymbol{I} \end{bmatrix}, \tag{52}$$

such as the consistent and lumped finite element mass matrix, commutes with any block-diagonal matrix of appropriate size, and is invariant under left- and right-multiplication, in the sense of Eq. (50)/Eq. (51), if the matrix composing the block-diagonal matrix is orthogonal and of appropriate size.

(ii) The continuous definition of the kinetic energy is given by Eq. (6)

$$\mathcal{T} = \frac{1}{2}\int_{\mathcal{V}} \rho\dot{\boldsymbol{\imath}}^{\mathrm{T}}\dot{\boldsymbol{\imath}}\,\mathrm{d}\mathcal{V}.$$

If we now look at the continuous version of the kinematic description stated in Eq. (1), i.e.,

$$\boldsymbol{\imath} = \boldsymbol{\tau} + \boldsymbol{A}\,(\overline{\boldsymbol{\jmath}} + \overline{\boldsymbol{c}}_{\mathrm{f}})\,,$$

with, Eq. (2),

$$\overline{c}_\mathrm{f} = \overline{\mathcal{S}}\,\overline{\boldsymbol{c}}_\mathrm{f},$$

see Sect. 2.2.1, and if we restrict ourselves to the aforementioned finite elements with identical shape functions $\overline{\mathcal{S}}$ used to interpolate all coordinate directions, i.e.,

$$\overline{\mathcal{S}} = \begin{bmatrix} S^{(1)}\boldsymbol{I} & \dots & S^{(n_\mathrm{n})}\boldsymbol{I} \end{bmatrix}, \tag{53}$$

and if we use the same shape functions to interpolate the geometry (isoparametric finite elements) the following expressions hold [90]

$$\overline{\mathcal{S}}\,(\mathbf{1}\otimes\boldsymbol{I}) \underset{(53)}{\overset{(43)}{=}} \boldsymbol{I} \quad \text{since} \quad \sum_{i=1}^{n_\mathrm{n}} S^{(i)} = 1, \tag{54}$$

$$\overline{\boldsymbol{x}} = \overline{\mathcal{S}}\overline{\boldsymbol{x}}, \tag{55}$$

$$\boldsymbol{A}\overline{\mathcal{S}} \underset{(53)}{\overset{(45)}{=}} \overline{\mathcal{S}}\boldsymbol{A}_\mathrm{bd}. \tag{56}$$

Hence,

$$\boldsymbol{\imath} = \overline{\mathcal{S}}\,(\mathbf{1}\otimes\boldsymbol{I})\,\boldsymbol{\tau} + \overline{\mathcal{S}}\boldsymbol{A}_\mathrm{bd}\,(\overline{\boldsymbol{x}} + \overline{\boldsymbol{c}}_\mathrm{f}) \tag{57}$$

$$= \overline{\mathcal{S}}\boldsymbol{r}, \tag{58}$$

which completes the proof, since substituting Eq. (58) into Eq. (6) and realizing that (Eq. (20))

$$\overline{\boldsymbol{M}} = \int_\mathcal{V} \rho\overline{\mathcal{S}}^\mathrm{T}\overline{\mathcal{S}}\,\mathrm{d}\mathcal{V}$$

yields Eq. (49). This simply implies that the aforementioned shape functions may be used to represent rigid body translation, rigid body rotation, and flexible deformation.

It is important to emphasize that the system energies defined in Eq. (48) and Eq. (49) are written in terms of nodal quantities and are therefore valid independent of the choice of generalized coordinates. However, it is clear that for any proper choice of generalized coordinates we can define functional relationships between the nodal quantities used to define the system energies and the generalized coordinates as

$$T = T(\dot{\boldsymbol{r}}(\boldsymbol{q},\dot{\boldsymbol{q}})), \tag{59}$$

and

$$U = U(\overline{\boldsymbol{c}}_\mathrm{f}(\boldsymbol{q})). \tag{60}$$

Eq. (59) deserves slightly more consideration. The nodal positions of all nodes are uniquely defined by the chosen generalized coordinates, in other words

$$\boldsymbol{r} = \boldsymbol{r}(\boldsymbol{q}). \tag{61}$$

Hence,

$$\dot{\boldsymbol{r}} = \frac{\partial \boldsymbol{r}}{\partial \boldsymbol{q}}\dot{\boldsymbol{q}} \tag{62}$$

$$= \dot{\boldsymbol{r}}\,(\boldsymbol{q},\dot{\boldsymbol{q}}) \tag{63}$$

since $\boldsymbol{q} = \boldsymbol{q}(t)$. From Eq. (62) it is also evident that

$$\frac{\partial \dot{\boldsymbol{r}}}{\partial \dot{\boldsymbol{q}}} = \frac{\partial \boldsymbol{r}}{\partial \boldsymbol{q}} = \boldsymbol{L}, \tag{64}$$

where $\boldsymbol{L}$ is the coordinate Jacobian of the nodal positions.

Hence, the force contributions according to Eq. (47) yield:

- Inertia forces [102]:

$$\frac{\mathrm{d}}{\mathrm{d}t}\left(\frac{\partial T}{\partial \dot{\boldsymbol{q}}^{\mathrm{T}}}\right) - \frac{\partial T}{\partial \boldsymbol{q}^{\mathrm{T}}} \overset{(59)}{=} \frac{\mathrm{d}}{\mathrm{d}t}\left(\frac{\partial \dot{\boldsymbol{r}}}{\partial \dot{\boldsymbol{q}}^{\mathrm{T}}}\frac{\partial T}{\partial \dot{\boldsymbol{r}}^{\mathrm{T}}}\right) - \frac{\partial \dot{\boldsymbol{r}}}{\partial \boldsymbol{q}^{\mathrm{T}}}\frac{\partial T}{\partial \dot{\boldsymbol{r}}^{\mathrm{T}}} \tag{65}$$

$$\overset{(49)}{=} \frac{\mathrm{d}}{\mathrm{d}t}\left(\frac{\partial \dot{\boldsymbol{r}}}{\partial \dot{\boldsymbol{q}}^{\mathrm{T}}}\overline{\boldsymbol{M}}\dot{\boldsymbol{r}}\right) - \frac{\mathrm{d}}{\mathrm{d}t}\left(\frac{\partial \boldsymbol{r}}{\partial \boldsymbol{q}^{\mathrm{T}}}\right)\overline{\boldsymbol{M}}\dot{\boldsymbol{r}} \tag{66}$$

$$\overset{(64)}{=} \frac{\mathrm{d}}{\mathrm{d}t}\left(\boldsymbol{L}^{\mathrm{T}}\overline{\boldsymbol{M}}\dot{\boldsymbol{r}}\right) - \frac{\mathrm{d}}{\mathrm{d}t}\left(\boldsymbol{L}^{\mathrm{T}}\right)\overline{\boldsymbol{M}}\dot{\boldsymbol{r}} \tag{67}$$

$$\overset{\substack{(62)\\(64)}}{=} \frac{\mathrm{d}}{\mathrm{d}t}\left(\boldsymbol{L}^{\mathrm{T}}\overline{\boldsymbol{M}}\boldsymbol{L}\dot{\boldsymbol{q}}\right) - \frac{\mathrm{d}}{\mathrm{d}t}\left(\boldsymbol{L}^{\mathrm{T}}\right)\overline{\boldsymbol{M}}\boldsymbol{L}\dot{\boldsymbol{q}} \tag{68}$$

$$= \dot{\boldsymbol{L}}^{\mathrm{T}}\overline{\boldsymbol{M}}\boldsymbol{L}\dot{\boldsymbol{q}} + \boldsymbol{L}^{\mathrm{T}}\overline{\boldsymbol{M}}\dot{\boldsymbol{L}}\dot{\boldsymbol{q}} + \boldsymbol{L}^{\mathrm{T}}\overline{\boldsymbol{M}}\boldsymbol{L}\ddot{\boldsymbol{q}} - \dot{\boldsymbol{L}}^{\mathrm{T}}\overline{\boldsymbol{M}}\boldsymbol{L}\dot{\boldsymbol{q}} \tag{69}$$

$$= \boldsymbol{L}^{\mathrm{T}}\overline{\boldsymbol{M}}\dot{\boldsymbol{L}}\dot{\boldsymbol{q}} + \boldsymbol{L}^{\mathrm{T}}\overline{\boldsymbol{M}}\boldsymbol{L}\ddot{\boldsymbol{q}} \tag{70}$$

  Here we have also used the chain and product rule of differentiation, the fact that the order of differentiation does not matter, and $\overline{\boldsymbol{M}} = \mathrm{const}$.

- Elastic forces:

$$\frac{\partial U}{\partial \boldsymbol{q}^{\mathrm{T}}} \overset{(60)}{=} \frac{\partial \overline{\boldsymbol{c}}_{\mathrm{f}}}{\partial \boldsymbol{q}^{\mathrm{T}}}\frac{\partial U}{\partial \overline{\boldsymbol{c}}_{\mathrm{f}}^{\mathrm{T}}} \tag{71}$$

$$\overset{(48)}{=} \boldsymbol{P}^{\mathrm{T}}\overline{\boldsymbol{K}}\overline{\boldsymbol{c}}_{\mathrm{f}}(\boldsymbol{q}), \tag{72}$$

  with the coordinate Jacobian of the flexible part of the nodal displacements

$$\boldsymbol{P} = \frac{\partial \overline{\boldsymbol{c}}_{\mathrm{f}}}{\partial \boldsymbol{q}}. \tag{73}$$

- Constraint forces:

$$\frac{\partial \boldsymbol{\lambda}^{\mathrm{T}}\boldsymbol{g}}{\partial \boldsymbol{q}^{\mathrm{T}}} = \frac{\partial \boldsymbol{g}}{\partial \boldsymbol{q}^{\mathrm{T}}}\boldsymbol{\lambda} \tag{74}$$

$$= \boldsymbol{J}^{\mathrm{T}}\boldsymbol{\lambda}, \tag{75}$$

  with the constraint Jacobian

$$\boldsymbol{J} = \frac{\partial \boldsymbol{g}}{\partial \boldsymbol{q}}. \tag{76}$$

- Applied forces:

$$\frac{\partial \boldsymbol{r}}{\partial \boldsymbol{q}^{\mathrm{T}}}\boldsymbol{f} \overset{(64)}{=} \boldsymbol{L}^{\mathrm{T}}\boldsymbol{f} \tag{77}$$

Finally, replacing the just derived force contributions Eqs. (65) to (77) in Lagrange's equation (47) reveals that the nodal-based equations of motion of linearly-elastic multibody systems modeled by Eqs. (48) to (49) for any choice of generalized coordinates are given by

$$\underbrace{\boldsymbol{L}^{\mathrm{T}}\overline{\boldsymbol{M}}\boldsymbol{L}}_{\widehat{\boldsymbol{M}}}\ddot{\boldsymbol{q}} + \underbrace{\boldsymbol{L}^{\mathrm{T}}\overline{\boldsymbol{M}}\dot{\boldsymbol{L}}\dot{\boldsymbol{q}}}_{-\widehat{\boldsymbol{Q}}_{\mathrm{v}}} + \underbrace{\boldsymbol{P}^{\mathrm{T}}\overline{\boldsymbol{K}}\overline{\boldsymbol{c}}_{\mathrm{f}}(\boldsymbol{q})}_{-\widehat{\boldsymbol{Q}}_{\mathrm{e}}} + \underbrace{\boldsymbol{J}^{\mathrm{T}}\boldsymbol{\lambda}}_{-\widehat{\boldsymbol{Q}}_{\mathrm{c}}} = \underbrace{\boldsymbol{L}^{\mathrm{T}}\boldsymbol{f}}_{\widehat{\boldsymbol{Q}}_{\mathrm{a}}}, \tag{78}$$

i.e., in the well-known and concise form,

$$\widehat{\boldsymbol{M}}\ddot{\boldsymbol{q}} = \widehat{\boldsymbol{Q}}, \tag{79}$$

with the overall generalized forces

$$\widehat{\boldsymbol{Q}} = \widehat{\boldsymbol{Q}}_{\mathrm{a}} + \widehat{\boldsymbol{Q}}_{\mathrm{c}} + \widehat{\boldsymbol{Q}}_{\mathrm{e}} + \widehat{\boldsymbol{Q}}_{\mathrm{v}}. \tag{80}$$

Summary of the main result of Sect. 2.3.2 – generic form of the equations of motion

The main result of this section, that will be used throughout this paper, is the generic form of the equations of motion (78) of linearly-elastic multibody systems modeled by Eqs. (48) to (49) for any choice of generalized coordinates $\boldsymbol{q}$ in terms of the constant mass $\overline{\boldsymbol{M}}$ and stiffness $\overline{\boldsymbol{K}}$ matrices from linear elastodynamics, i.e., restated here for presentation purposes,

$$\boldsymbol{L}^{\mathrm{T}}\overline{\boldsymbol{M}}\boldsymbol{L}\ddot{\boldsymbol{q}} + \boldsymbol{L}^{\mathrm{T}}\overline{\boldsymbol{M}}\dot{\boldsymbol{L}}\dot{\boldsymbol{q}} + \boldsymbol{P}^{\mathrm{T}}\overline{\boldsymbol{K}}\overline{\boldsymbol{c}}_{\mathrm{f}}(\boldsymbol{q}) + \boldsymbol{J}^{\mathrm{T}}\boldsymbol{\lambda} = \boldsymbol{L}^{\mathrm{T}}\boldsymbol{f}$$

where again

$$\boldsymbol{L} = \frac{\partial \boldsymbol{r}}{\partial \boldsymbol{q}}, \quad \boldsymbol{P} = \frac{\partial \overline{\boldsymbol{c}}_{\mathrm{f}}}{\partial \boldsymbol{q}}, \quad \boldsymbol{J} = \frac{\partial \boldsymbol{g}}{\partial \boldsymbol{q}},$$

are coordinate and constraint Jacobians; here, $\boldsymbol{f}$ and $\boldsymbol{\lambda}$ represents the applied nodal forces and Lagrange multipliers, respectively, see also the summary of Sect. 2.3.1 for a description of the kinematic quantities. Hence, to define a linearly-elastic multibody formulation the following steps are sufficient:

1. Choose the generalized coordinates $\boldsymbol{q}$ – this choice defines the formulation.
2. Define the coordinate mappings $\boldsymbol{r} = \boldsymbol{r}(\boldsymbol{q})$ and $\overline{\boldsymbol{c}}_{\mathrm{f}} = \overline{\boldsymbol{c}}_{\mathrm{f}}(\boldsymbol{q})$.
3. Calculate the Jacobians of the coordinate mappings, i.e., $\boldsymbol{L}$ and $\boldsymbol{P}$.
4. Calculate the time derivative of $\boldsymbol{L}$, i.e., $\dot{\boldsymbol{L}}$.
5. Perform the matrix multiplications to obtain the final equations of motion.

These steps will be employed to derive the nodal-based equations of motion of the following linearly-elastic multibody formulations.

2.3.3 Nodal-based floating frame of reference formulation

Following the recipe outlined in Sect. 2.3.2 we now derive the nodal-based, i.e., inertia-shape-integral-free, FFRF equations of motion, initially proposed by [102, 90].

The first step is the definition of the generalized coordinates; for one body in the FFRF the coordinates are given by (see Sect. 2.3.1)

$$\boldsymbol{q} = \begin{bmatrix} \boldsymbol{\tau} \\ \boldsymbol{\theta} \\ \overline{\boldsymbol{c}}_{\mathrm{f}} \end{bmatrix},$$

which, of course, coincide with the coordinates of the conventional FFRF, see Eq. (5).

The second step involves the definition of the coordinate mappings used to define the system energies stated in Eqs. (48) to (49). It is trivial to extract the flexible local nodal displacements from the FFRF generalized coordinates with a Boolean matrix $\boldsymbol{B}$, i.e.,

$$\overline{\boldsymbol{c}}_{\mathrm{f}} = \boldsymbol{B}\boldsymbol{q}, \tag{81}$$

where

$$\boldsymbol{B} = \begin{bmatrix} \boldsymbol{0}_{3n_{\mathrm{n}}\times 3} & \boldsymbol{0}_{3n_{\mathrm{n}}\times n_{\mathrm{r}}} & \boldsymbol{I}_{3n_{\mathrm{n}}\times 3n_{\mathrm{n}}} \end{bmatrix}. \tag{82}$$

Hence, the corresponding coordinate Jacobian follows as

$$\boldsymbol{P} = \boldsymbol{B}. \tag{83}$$

Given the FFRF generalized coordinates, we now see that Eq. (42) represents the desired mapping stated in Eq. (61), since $\boldsymbol{A}_{\mathrm{bd}} = \boldsymbol{A}_{\mathrm{bd}}(\boldsymbol{A}(\boldsymbol{\theta}))$. Hence, the corresponding Jacobian may be calculated as

$$\frac{\partial \boldsymbol{r}}{\partial \boldsymbol{q}} = \begin{bmatrix} \frac{\partial \boldsymbol{r}}{\partial \boldsymbol{\tau}} & \frac{\partial \boldsymbol{r}}{\partial \boldsymbol{\theta}} & \frac{\partial \boldsymbol{r}}{\partial \overline{\boldsymbol{c}}_{\mathrm{f}}} \end{bmatrix}, \tag{84}$$

which yields [102]

$$\boldsymbol{L} = \begin{bmatrix} (\mathbf{1} \otimes \boldsymbol{I}) & -\boldsymbol{A}_{\mathrm{bd}} \widetilde{\overline{\boldsymbol{r}}}_{\mathrm{f}} \overline{\boldsymbol{G}} & \boldsymbol{A}_{\mathrm{bd}} \end{bmatrix}. \tag{85}$$

Here we use the tilde operator to define the matrix $\widetilde{\overline{\boldsymbol{r}}}_{\mathrm{f}}$, which is composed by n_{n} skew-symmetric matrices $\widetilde{\overline{\boldsymbol{r}}}_{\mathrm{f}}^{(i)} \in \mathbb{R}^{3\times 3}$, i.e.,

$$\widetilde{\overline{\boldsymbol{r}}}_{\mathrm{f}} = \begin{bmatrix} \widetilde{\overline{\boldsymbol{r}}}_{\mathrm{f}}^{(1)} \\ \vdots \\ \widetilde{\overline{\boldsymbol{r}}}_{\mathrm{f}}^{(n_{\mathrm{n}})} \end{bmatrix} \in \mathbb{R}^{3n_{\mathrm{n}}\times 3}, \tag{86}$$

where the local nodal positions $\overline{\boldsymbol{r}}_{\mathrm{f}}^{(i)}$ and the system matrix of nodal positions $\overline{\boldsymbol{r}}_{\mathrm{f}}$ are given by (Fig. 2)

$$\overline{\boldsymbol{r}}_{\mathrm{f}}^{(i)} = \overline{\boldsymbol{x}}^{(i)} + \overline{\boldsymbol{c}}_{\mathrm{f}}^{(i)} \in \mathbb{R}^{3\times 1} \;\Leftrightarrow\; \overline{\boldsymbol{r}}_{\mathrm{f}} = \overline{\boldsymbol{x}} + \overline{\boldsymbol{c}}_{\mathrm{f}} \in \mathbb{R}^{3n_{\mathrm{n}}\times 1}. \tag{87}$$

Furthermore, Eq. (15) has been applied to the nodal structure of the equations to obtain Eq. (85).

The last ingredient required is the time derivative of $\boldsymbol{L}$, i.e.,

$$\dot{\boldsymbol{L}} = \begin{bmatrix} \mathbf{0}_{3n_{\mathrm{n}}\times 3} & -\boldsymbol{A}_{\mathrm{bd}} \left(\widetilde{\overline{\boldsymbol{\omega}}}_{\mathrm{bd}} \widetilde{\overline{\boldsymbol{r}}}_{\mathrm{f}} \overline{\boldsymbol{G}} + \dot{\widetilde{\overline{\boldsymbol{c}}}}_{\mathrm{f}} \overline{\boldsymbol{G}} + \widetilde{\overline{\boldsymbol{r}}}_{\mathrm{f}} \dot{\overline{\boldsymbol{G}}} \right) & \boldsymbol{A}_{\mathrm{bd}} \widetilde{\overline{\boldsymbol{\omega}}}_{\mathrm{bd}} \end{bmatrix}, \tag{88}$$

since $\overline{\boldsymbol{x}} = \mathrm{const.}$ (see Eq. (87)) and

$$\dot{\boldsymbol{A}} = \boldsymbol{A} \widetilde{\overline{\boldsymbol{\omega}}} \quad \Rightarrow \quad \dot{\boldsymbol{A}}_{\mathrm{bd}} = \boldsymbol{A}_{\mathrm{bd}} \widetilde{\overline{\boldsymbol{\omega}}}_{\mathrm{bd}} \tag{89}$$

where

$$\widetilde{\overline{\boldsymbol{\omega}}}_{\mathrm{bd}} = \mathrm{diag}(\widetilde{\overline{\boldsymbol{\omega}}}, \ldots, \widetilde{\overline{\boldsymbol{\omega}}}) \in \mathbb{R}^{3n_{\mathrm{n}}\times 3n_{\mathrm{n}}} \tag{90}$$

denotes the block diagonal matrix of skew-symmetric local angular velocity vectors.

Finally, according to Eq. (78), we obtain (see also the summary at the end of Sect. 2.3.2)

$$\begin{aligned}
&\begin{bmatrix} (\mathbf{1} \otimes \boldsymbol{I})^{\mathrm{T}} \overline{\boldsymbol{M}} (\mathbf{1} \otimes \boldsymbol{I}) & -\boldsymbol{A} (\mathbf{1} \otimes \boldsymbol{I})^{\mathrm{T}} \overline{\boldsymbol{M}} \widetilde{\overline{\boldsymbol{r}}}_{\mathrm{f}} \overline{\boldsymbol{G}} & \boldsymbol{A} (\mathbf{1} \otimes \boldsymbol{I})^{\mathrm{T}} \overline{\boldsymbol{M}} \\ & \overline{\boldsymbol{G}}^{\mathrm{T}} \widetilde{\overline{\boldsymbol{r}}}_{\mathrm{f}}^{\mathrm{T}} \overline{\boldsymbol{M}} \widetilde{\overline{\boldsymbol{r}}}_{\mathrm{f}} \overline{\boldsymbol{G}} & -\overline{\boldsymbol{G}}^{\mathrm{T}} \widetilde{\overline{\boldsymbol{r}}}_{\mathrm{f}}^{\mathrm{T}} \overline{\boldsymbol{M}} \\ \text{sym.} & & \overline{\boldsymbol{M}} \end{bmatrix} \begin{bmatrix} \ddot{\boldsymbol{\tau}} \\ \ddot{\boldsymbol{\theta}} \\ \ddot{\overline{\boldsymbol{c}}}_{\mathrm{f}} \end{bmatrix} = - \begin{bmatrix} \mathbf{0}_{3\times 3} & & \\ & \mathbf{0}_{n_{\mathrm{r}}\times n_{\mathrm{r}}} & \\ & & \overline{\boldsymbol{K}} \end{bmatrix} \begin{bmatrix} \boldsymbol{\tau} \\ \boldsymbol{\theta} \\ \overline{\boldsymbol{c}}_{\mathrm{f}} \end{bmatrix} \\
&+ \begin{bmatrix} -\boldsymbol{A} (\mathbf{1} \otimes \boldsymbol{I})^{\mathrm{T}} \overline{\boldsymbol{M}} \left(\widetilde{\overline{\boldsymbol{\omega}}}_{\mathrm{bd}} \widetilde{\overline{\boldsymbol{\omega}}}_{\mathrm{bd}} \overline{\boldsymbol{r}}_{\mathrm{f}} + 2 \widetilde{\overline{\boldsymbol{\omega}}}_{\mathrm{bd}} \dot{\overline{\boldsymbol{c}}}_{\mathrm{f}} - \widetilde{\overline{\boldsymbol{r}}}_{\mathrm{f}} \dot{\overline{\boldsymbol{G}}} \dot{\boldsymbol{\theta}} \right) \\ \overline{\boldsymbol{G}}^{\mathrm{T}} \widetilde{\overline{\boldsymbol{r}}}_{\mathrm{f}}^{\mathrm{T}} \overline{\boldsymbol{M}} \left(\widetilde{\overline{\boldsymbol{\omega}}}_{\mathrm{bd}} \widetilde{\overline{\boldsymbol{\omega}}}_{\mathrm{bd}} \overline{\boldsymbol{r}}_{\mathrm{f}} + 2 \widetilde{\overline{\boldsymbol{\omega}}}_{\mathrm{bd}} \dot{\overline{\boldsymbol{c}}}_{\mathrm{f}} - \widetilde{\overline{\boldsymbol{r}}}_{\mathrm{f}} \dot{\overline{\boldsymbol{G}}} \dot{\boldsymbol{\theta}} \right) \\ -\overline{\boldsymbol{M}} \left(\widetilde{\overline{\boldsymbol{\omega}}}_{\mathrm{bd}} \widetilde{\overline{\boldsymbol{\omega}}}_{\mathrm{bd}} \overline{\boldsymbol{r}}_{\mathrm{f}} + 2 \widetilde{\overline{\boldsymbol{\omega}}}_{\mathrm{bd}} \dot{\overline{\boldsymbol{c}}}_{\mathrm{f}} - \widetilde{\overline{\boldsymbol{r}}}_{\mathrm{f}} \dot{\overline{\boldsymbol{G}}} \dot{\boldsymbol{\theta}} \right) \end{bmatrix} \\
&+ \begin{bmatrix} (\mathbf{1} \otimes \boldsymbol{I})^{\mathrm{T}} \\ -\overline{\boldsymbol{G}}^{\mathrm{T}} \widetilde{\overline{\boldsymbol{r}}}_{\mathrm{f}}^{\mathrm{T}} \boldsymbol{A}_{\mathrm{bd}}^{\mathrm{T}} \\ \boldsymbol{A}_{\mathrm{bd}}^{\mathrm{T}} \end{bmatrix} \boldsymbol{f} - \frac{\partial \boldsymbol{g}}{\partial \boldsymbol{q}^{\mathrm{T}}} \boldsymbol{\lambda},
\end{aligned} \tag{91}$$

where

$$\boldsymbol{A}_{\mathrm{bd}}^{\mathrm{T}} \boldsymbol{A}_{\mathrm{bd}} = \boldsymbol{I}_{\mathrm{bd}}, \tag{92}$$

$$(\mathbf{1} \otimes \boldsymbol{I})^{\mathrm{T}} \boldsymbol{A}_{\mathrm{bd}} = \boldsymbol{A} (\mathbf{1} \otimes \boldsymbol{I})^{\mathrm{T}}, \tag{93}$$

$$\widetilde{\overline{\boldsymbol{\omega}}}_{\mathrm{bd}} \overline{\boldsymbol{r}}_{\mathrm{f}} = -\widetilde{\overline{\boldsymbol{r}}}_{\mathrm{f}} \overline{\boldsymbol{\omega}} \quad \text{(true for any nodal quantity arranged according to Eq. (46))}, \tag{94}$$

and Eq. (51) as well as Eq. (13) have been used to simplify the expression.

It shall be emphasized that the nodal-based Eq. (91) does not include any shape integrals, but still is fully consistent with respect to the nodal interpolation of the underlying finite elements. In addition, this formulation does not use lumped mass approximations and is, to our knowledge, the only consistent formulation without the well-known inertia shape integrals [31].

2.3.4 Nodal-based component mode synthesis floating frame of reference formulation

As already mentioned in Sect. 2.2.2 the FFRF is usually employed with modal reduction to reduce the number of flexible generalized coordinates. Therefore, the CMS-FFRF generalized coordinates are given by

$$\boldsymbol{q} = \begin{bmatrix} \boldsymbol{\tau} \\ \boldsymbol{\theta} \\ \boldsymbol{\zeta} \end{bmatrix}. \tag{95}$$

Hence, the extraction of the flexible nodal-displacements from the generalized coordinates requires in addition to the Boolean matrix used before (Eq. (82)) the reduction basis, i.e.,

$$\overline{\boldsymbol{c}}_{\mathrm{f}} = \overline{\boldsymbol{\Psi}} \boldsymbol{B} \boldsymbol{q}. \tag{96}$$

The corresponding coordinate Jacobian then follows as

$$\boldsymbol{P} = \overline{\boldsymbol{\Psi}} \boldsymbol{B}. \tag{97}$$

For the nodal positions of all nodes we simply substitute the modal ansatz from Eq. (22) into Eq. (42), hence

$$\boldsymbol{r} = (\boldsymbol{1} \otimes \boldsymbol{I})\, \boldsymbol{\tau} + \boldsymbol{A}_{\mathrm{bd}} \left(\overline{\boldsymbol{x}} + \overline{\boldsymbol{\Psi}} \boldsymbol{\zeta} \right). \tag{98}$$

Following now the same steps outlined in the previous section, where we have derived the unreduced FFRF equations of motion, yields

$$\boldsymbol{L} = \begin{bmatrix} (\boldsymbol{1} \otimes \boldsymbol{I}) & -\boldsymbol{A}_{\mathrm{bd}} \widetilde{\overline{\boldsymbol{r}}}_{\mathrm{f}} \overline{\boldsymbol{G}} & \boldsymbol{A}_{\mathrm{bd}} \overline{\boldsymbol{\Psi}} \end{bmatrix}, \tag{99}$$

and

$$\dot{\boldsymbol{L}} = \begin{bmatrix} \boldsymbol{0}_{3n_{\mathrm{n}} \times 3} & -\boldsymbol{A}_{\mathrm{bd}} \left(\widetilde{\overline{\boldsymbol{\omega}}}_{\mathrm{bd}} \widetilde{\overline{\boldsymbol{r}}}_{\mathrm{f}} \overline{\boldsymbol{G}} + \dot{\widetilde{\overline{\boldsymbol{c}}}}_{\mathrm{f}} \overline{\boldsymbol{G}} + \widetilde{\overline{\boldsymbol{r}}}_{\mathrm{f}} \dot{\overline{\boldsymbol{G}}} \right) & \boldsymbol{A}_{\mathrm{bd}} \widetilde{\overline{\boldsymbol{\omega}}}_{\mathrm{bd}} \overline{\boldsymbol{\Psi}} \end{bmatrix}, \tag{100}$$

and finally

$$\begin{aligned}
&\begin{bmatrix} (\boldsymbol{1} \otimes \boldsymbol{I})^{\mathrm{T}} \overline{\boldsymbol{M}} (\boldsymbol{1} \otimes \boldsymbol{I}) & -\boldsymbol{A} (\boldsymbol{1} \otimes \boldsymbol{I})^{\mathrm{T}} \overline{\boldsymbol{M}} \widetilde{\overline{\boldsymbol{r}}}_{\mathrm{f}} \overline{\boldsymbol{G}} & \boldsymbol{A} (\boldsymbol{1} \otimes \boldsymbol{I})^{\mathrm{T}} \overline{\boldsymbol{M}} \overline{\boldsymbol{\Psi}} \\ & \overline{\boldsymbol{G}}^{\mathrm{T}} \widetilde{\overline{\boldsymbol{r}}}_{\mathrm{f}}^{\mathrm{T}} \overline{\boldsymbol{M}} \widetilde{\overline{\boldsymbol{r}}}_{\mathrm{f}} \overline{\boldsymbol{G}} & -\overline{\boldsymbol{G}}^{\mathrm{T}} \widetilde{\overline{\boldsymbol{r}}}_{\mathrm{f}}^{\mathrm{T}} \overline{\boldsymbol{M}} \overline{\boldsymbol{\Psi}} \\ \text{sym.} & & \overline{\boldsymbol{\Psi}}^{\mathrm{T}} \overline{\boldsymbol{M}} \overline{\boldsymbol{\Psi}} \end{bmatrix} \begin{bmatrix} \ddot{\boldsymbol{\tau}} \\ \ddot{\boldsymbol{\theta}} \\ \ddot{\boldsymbol{\zeta}} \end{bmatrix} = - \begin{bmatrix} \boldsymbol{0}_{3\times 3} & & \\ & \boldsymbol{0}_{n_{\mathrm{r}} \times n_{\mathrm{r}}} & \\ & & \overline{\boldsymbol{\Psi}}^{\mathrm{T}} \overline{\boldsymbol{K}} \overline{\boldsymbol{\Psi}} \end{bmatrix} \begin{bmatrix} \boldsymbol{\tau} \\ \boldsymbol{\theta} \\ \boldsymbol{\zeta} \end{bmatrix} \\
&+ \begin{bmatrix} -\boldsymbol{A} (\boldsymbol{1} \otimes \boldsymbol{I})^{\mathrm{T}} \overline{\boldsymbol{M}} \left(\widetilde{\overline{\boldsymbol{\omega}}}_{\mathrm{bd}} \widetilde{\overline{\boldsymbol{\omega}}}_{\mathrm{bd}} \overline{\boldsymbol{r}}_{\mathrm{f}} + 2 \widetilde{\overline{\boldsymbol{\omega}}}_{\mathrm{bd}} \dot{\overline{\boldsymbol{c}}}_{\mathrm{f}} - \widetilde{\overline{\boldsymbol{r}}}_{\mathrm{f}} \dot{\overline{\boldsymbol{G}}} \dot{\boldsymbol{\theta}} \right) \\ \overline{\boldsymbol{G}}^{\mathrm{T}} \widetilde{\overline{\boldsymbol{r}}}_{\mathrm{f}}^{\mathrm{T}} \overline{\boldsymbol{M}} \left(\widetilde{\overline{\boldsymbol{\omega}}}_{\mathrm{bd}} \widetilde{\overline{\boldsymbol{\omega}}}_{\mathrm{bd}} \overline{\boldsymbol{r}}_{\mathrm{f}} + 2 \widetilde{\overline{\boldsymbol{\omega}}}_{\mathrm{bd}} \dot{\overline{\boldsymbol{c}}}_{\mathrm{f}} - \widetilde{\overline{\boldsymbol{r}}}_{\mathrm{f}} \dot{\overline{\boldsymbol{G}}} \dot{\boldsymbol{\theta}} \right) \\ -\overline{\boldsymbol{\Psi}}^{\mathrm{T}} \overline{\boldsymbol{M}} \left(\widetilde{\overline{\boldsymbol{\omega}}}_{\mathrm{bd}} \widetilde{\overline{\boldsymbol{\omega}}}_{\mathrm{bd}} \overline{\boldsymbol{r}}_{\mathrm{f}} + 2 \widetilde{\overline{\boldsymbol{\omega}}}_{\mathrm{bd}} \dot{\overline{\boldsymbol{c}}}_{\mathrm{f}} - \widetilde{\overline{\boldsymbol{r}}}_{\mathrm{f}} \dot{\overline{\boldsymbol{G}}} \dot{\boldsymbol{\theta}} \right) \end{bmatrix} \\
&+ \begin{bmatrix} (\boldsymbol{1} \otimes \boldsymbol{I})^{\mathrm{T}} \\ -\overline{\boldsymbol{G}}^{\mathrm{T}} \widetilde{\overline{\boldsymbol{r}}}_{\mathrm{f}}^{\mathrm{T}} \boldsymbol{A}_{\mathrm{bd}}^{\mathrm{T}} \\ \overline{\boldsymbol{\Psi}}^{\mathrm{T}} \boldsymbol{A}_{\mathrm{bd}}^{\mathrm{T}} \end{bmatrix} \boldsymbol{f} - \frac{\partial \boldsymbol{g}}{\partial \boldsymbol{q}^{\mathrm{T}}} \boldsymbol{\lambda}.
\end{aligned} \tag{101}$$

The modally-reduced FFRF mass sub-matrices $\widehat{\boldsymbol{M}}_{ij}$ and quadratic velocity vector components $\widehat{\boldsymbol{Q}}_{\mathrm{v}_i}$ need slightly more considerations to bring them in a form usually employed by multibody dynamicists. The aim of the following rearrangements is to avoid the "large" matrix multiplications still involved in Eq. (101) by making sure that the unreduced finite element mass matrix always "meets" a rectangular matrix on each side to reduce the sizes of all equation terms. To this end, the quadratic velocity vector may be rearranged as, see [104] for details regarding the rest of this section,

$$\widehat{\boldsymbol{Q}}_{\mathrm{v}} = \begin{bmatrix} \boldsymbol{A} \left(\widetilde{\overline{\boldsymbol{\omega}}} (\boldsymbol{1} \otimes \boldsymbol{I})^{\mathrm{T}} \overline{\boldsymbol{M}} \widetilde{\overline{\boldsymbol{r}}}_{\mathrm{f}} \overline{\boldsymbol{\omega}} + 2 (\boldsymbol{1} \otimes \boldsymbol{I})^{\mathrm{T}} \overline{\boldsymbol{M}} \dot{\widetilde{\overline{\boldsymbol{c}}}}_{\mathrm{f}} \overline{\boldsymbol{\omega}} + (\boldsymbol{1} \otimes \boldsymbol{I})^{\mathrm{T}} \overline{\boldsymbol{M}} \widetilde{\overline{\boldsymbol{r}}}_{\mathrm{f}} \dot{\overline{\boldsymbol{G}}} \dot{\boldsymbol{\theta}} \right) \\ -\overline{\boldsymbol{G}}^{\mathrm{T}} \left(\widetilde{\overline{\boldsymbol{\omega}}} \widetilde{\overline{\boldsymbol{r}}}_{\mathrm{f}}^{\mathrm{T}} \overline{\boldsymbol{M}} \widetilde{\overline{\boldsymbol{r}}}_{\mathrm{f}} \overline{\boldsymbol{\omega}} + 2 \dot{\widetilde{\overline{\boldsymbol{r}}}}_{\mathrm{f}}^{\mathrm{T}} \overline{\boldsymbol{M}} \dot{\widetilde{\overline{\boldsymbol{c}}}}_{\mathrm{f}} \overline{\boldsymbol{\omega}} + \widetilde{\overline{\boldsymbol{r}}}_{\mathrm{f}}^{\mathrm{T}} \overline{\boldsymbol{M}} \widetilde{\overline{\boldsymbol{r}}}_{\mathrm{f}} \dot{\overline{\boldsymbol{G}}} \dot{\boldsymbol{\theta}} \right) \\ (\boldsymbol{I}_{\zeta} \otimes \overline{\boldsymbol{\omega}})^{\mathrm{T}} \widetilde{\overline{\boldsymbol{\Psi}}}^{\mathrm{T}} \overline{\boldsymbol{M}} \widetilde{\overline{\boldsymbol{r}}}_{\mathrm{f}} \overline{\boldsymbol{\omega}} + 2 \overline{\boldsymbol{\Psi}}^{\mathrm{T}} \overline{\boldsymbol{M}} \dot{\widetilde{\overline{\boldsymbol{c}}}}_{\mathrm{f}} \overline{\boldsymbol{\omega}} + \overline{\boldsymbol{\Psi}}^{\mathrm{T}} \overline{\boldsymbol{M}} \widetilde{\overline{\boldsymbol{r}}}_{\mathrm{f}} \dot{\overline{\boldsymbol{G}}} \dot{\boldsymbol{\theta}} \end{bmatrix}, \end{bmatrix} \tag{102}$$

with an identity matrix $\boldsymbol{I}_\zeta \in \mathbb{R}^{n_\mathrm{m} \times n_\mathrm{m}}$ of proper size, and where

$$\widetilde{\overline{\boldsymbol{\Psi}}} = \begin{bmatrix} \widetilde{\overline{\boldsymbol{\psi}}}_1 & \dots & \widetilde{\overline{\boldsymbol{\psi}}}_{n_\mathrm{m}} \end{bmatrix} \in \mathbb{R}^{3n_\mathrm{n} \times 3n_\mathrm{m}} \tag{103}$$

with $\widetilde{\overline{\boldsymbol{\psi}}}_m \in \mathbb{R}^{3n_\mathrm{n} \times 3}$ denoting the corresponding matrix generated from component mode $\overline{\boldsymbol{\psi}}_m$ according to Eq. (86). The matrix $\widetilde{\overline{\boldsymbol{\Psi}}}$ is also employed to express the skew-symmetric flexible nodal displacements in terms of the modal coordinates and modes, i.e.,

$$\widetilde{\overline{\boldsymbol{c}}}_\mathrm{f} = \widetilde{\overline{\boldsymbol{\Psi}}} (\boldsymbol{\zeta} \otimes \boldsymbol{I}). \tag{104}$$

Now all preparations are made to reduce the size of the governing equations via the introduction of the nodal-based FFRF invariants, which are "small" and constant matrices describing the inertia and flexibility distribution of the body – some having clear physical interpretations; the total mass of the body m is calculated from the quantities arising in the rearranged equations as

$$m\boldsymbol{I} = (\boldsymbol{1} \otimes \boldsymbol{I})^\mathrm{T} \, \overline{\boldsymbol{M}} \, (\boldsymbol{1} \otimes \boldsymbol{I}) \in \mathbb{R}^{3\times 3}. \tag{105}$$

Likewise, the center of mass position of the undeformed body $\overline{\boldsymbol{\chi}}_\mathrm{u}$ with respect to the floating frame is obtained via

$$\overline{\boldsymbol{\chi}}_\mathrm{u} = \frac{1}{m} (\boldsymbol{1} \otimes \boldsymbol{I})^\mathrm{T} \, \overline{\boldsymbol{M}} \, \overline{\boldsymbol{x}} \in \mathbb{R}^{3\times 1}, \tag{106}$$

and the inertia tensor of the undeformed body $\overline{\boldsymbol{\Theta}}_\mathrm{u}$ expressed in the floating frame is given by

$$\overline{\boldsymbol{\Theta}}_\mathrm{u} = \widetilde{\overline{\boldsymbol{x}}}^\mathrm{T} \overline{\boldsymbol{M}} \, \widetilde{\overline{\boldsymbol{x}}} \in \mathbb{R}^{3\times 3}. \tag{107}$$

Furthermore, we can define the remaining FFRF invariants:

$$\overline{\boldsymbol{M}}_{\psi\psi} = \overline{\boldsymbol{\Psi}}^\mathrm{T} \overline{\boldsymbol{M}} \, \overline{\boldsymbol{\Psi}} \in \mathbb{R}^{n_\mathrm{m} \times n_\mathrm{m}}, \tag{108}$$

$$\overline{\boldsymbol{M}}_{\widetilde{\psi}\psi} = \widetilde{\overline{\boldsymbol{\Psi}}}^\mathrm{T} \overline{\boldsymbol{M}} \, \overline{\boldsymbol{\Psi}} \in \mathbb{R}^{3n_\mathrm{m} \times n_\mathrm{m}}, \tag{109}$$

$$\overline{\boldsymbol{M}}_{\widetilde{\psi}\widetilde{\psi}} = \widetilde{\overline{\boldsymbol{\Psi}}}^\mathrm{T} \overline{\boldsymbol{M}} \, \widetilde{\overline{\boldsymbol{\Psi}}} \in \mathbb{R}^{3n_\mathrm{m} \times 3n_\mathrm{m}}, \tag{110}$$

$$\overline{\boldsymbol{M}}_{\phi\psi} = (\boldsymbol{1} \otimes \boldsymbol{I})^\mathrm{T} \overline{\boldsymbol{M}} \, \overline{\boldsymbol{\Psi}} \in \mathbb{R}^{3 \times n_\mathrm{m}}, \tag{111}$$

$$\overline{\boldsymbol{M}}_{\phi\widetilde{\psi}} = (\boldsymbol{1} \otimes \boldsymbol{I})^\mathrm{T} \overline{\boldsymbol{M}} \, \widetilde{\overline{\boldsymbol{\Psi}}} \in \mathbb{R}^{3 \times 3n_\mathrm{m}}, \tag{112}$$

$$\overline{\boldsymbol{M}}_{\widetilde{x}\psi} = \widetilde{\overline{\boldsymbol{x}}}^\mathrm{T} \overline{\boldsymbol{M}} \, \overline{\boldsymbol{\Psi}} \in \mathbb{R}^{3 \times n_\mathrm{m}}, \tag{113}$$

$$\overline{\boldsymbol{M}}_{\widetilde{x}\widetilde{\psi}} = \widetilde{\overline{\boldsymbol{x}}}^\mathrm{T} \overline{\boldsymbol{M}} \, \widetilde{\overline{\boldsymbol{\Psi}}} \in \mathbb{R}^{3 \times 3n_\mathrm{m}}, \tag{114}$$

where the first matrix (Eq. (108)) is the reduced finite element mass matrix known from linear elastodynamics. These constant matrices from Eqs. (105) to (114) represent the nodal-based FFRF invariants without integrals and without a lumped mass approach, which is usually employed by commercial multibody codes, see, e.g., [72, 71]. Using a lumped mass matrix to calculate these invariants leads to the invariants employed by commercial codes, see also Sect. 2.2.

Hence, the nodal-based CMS-FFRF mass sub-matrices read

$$\widehat{\boldsymbol{M}}_\mathrm{tt} = m\boldsymbol{I} \tag{115}$$

$$\widehat{\boldsymbol{M}}_\mathrm{ff} = \overline{\boldsymbol{M}}_{\psi\psi} \tag{116}$$

$$\widehat{\boldsymbol{M}}_\mathrm{tf} = \boldsymbol{A} \overline{\boldsymbol{M}}_{\phi\psi}, \tag{117}$$

$$\widehat{\boldsymbol{M}}_\mathrm{tr} = -\boldsymbol{A} \left[m\widetilde{\overline{\boldsymbol{\chi}}}_\mathrm{u} + \overline{\boldsymbol{M}}_{\phi\widetilde{\psi}} (\boldsymbol{\zeta} \otimes \boldsymbol{I}) \right] \overline{\boldsymbol{G}}, \tag{118}$$

$$\widehat{\boldsymbol{M}}_\mathrm{rf} = -\overline{\boldsymbol{G}}^\mathrm{T} \left[\overline{\boldsymbol{M}}_{\widetilde{x}\psi} + (\boldsymbol{\zeta} \otimes \boldsymbol{I})^\mathrm{T} \overline{\boldsymbol{M}}_{\widetilde{\psi}\psi} \right], \tag{119}$$

$$\widehat{\boldsymbol{M}}_\mathrm{rr} = \overline{\boldsymbol{G}}^\mathrm{T} \left[\overline{\boldsymbol{\Theta}}_\mathrm{u} + \overline{\boldsymbol{M}}_{\widetilde{x}\widetilde{\psi}} (\boldsymbol{\zeta} \otimes \boldsymbol{I}) + (\boldsymbol{\zeta} \otimes \boldsymbol{I})^\mathrm{T} \overline{\boldsymbol{M}}_{\widetilde{x}\widetilde{\psi}}^\mathrm{T} + (\boldsymbol{\zeta} \otimes \boldsymbol{I})^\mathrm{T} \overline{\boldsymbol{M}}_{\widetilde{\psi}\widetilde{\psi}} (\boldsymbol{\zeta} \otimes \boldsymbol{I}) \right] \overline{\boldsymbol{G}}, \tag{120}$$

and the nodal-based CMS-FFRF quadratic velocity vector components,

$$\begin{aligned}\widehat{\boldsymbol{Q}}_{\mathrm{v_t}} =& A\widetilde{\overline{\boldsymbol{\omega}}}\left[m\widetilde{\overline{\boldsymbol{\chi}}}_{\mathrm{u}} + \overline{\boldsymbol{M}}_{\phi\widetilde{\psi}}\left(\boldsymbol{\zeta}\otimes\boldsymbol{I}\right)\right]\overline{\boldsymbol{\omega}} + 2A\overline{\boldsymbol{M}}_{\phi\widetilde{\psi}}\left(\dot{\boldsymbol{\zeta}}\otimes\boldsymbol{I}\right)\overline{\boldsymbol{\omega}} \\ &+ \underbrace{A\left[m\widetilde{\overline{\boldsymbol{\chi}}}_{\mathrm{u}} + \overline{\boldsymbol{M}}_{\phi\widetilde{\psi}}\left(\boldsymbol{\zeta}\otimes\boldsymbol{I}\right)\right]\dot{\overline{\boldsymbol{G}}}\dot{\boldsymbol{\theta}}}_{\text{null if Euler parameters are used [31]}},\end{aligned} \tag{121}$$

$$\begin{aligned}\widehat{\boldsymbol{Q}}_{\mathrm{v_r}} =& -\overline{\boldsymbol{G}}^{\mathrm{T}}\widetilde{\overline{\boldsymbol{\omega}}}\left[\overline{\boldsymbol{\Theta}}_{\mathrm{u}} + \overline{\boldsymbol{M}}_{\widetilde{x}\widetilde{\psi}}\left(\boldsymbol{\zeta}\otimes\boldsymbol{I}\right) + \left(\boldsymbol{\zeta}\otimes\boldsymbol{I}\right)^{\mathrm{T}}\overline{\boldsymbol{M}}^{\mathrm{T}}_{\widetilde{x}\widetilde{\psi}} + \left(\boldsymbol{\zeta}\otimes\boldsymbol{I}\right)^{\mathrm{T}}\overline{\boldsymbol{M}}_{\widetilde{\psi}\widetilde{\psi}}\left(\boldsymbol{\zeta}\otimes\boldsymbol{I}\right)\right]\overline{\boldsymbol{\omega}} \\ &- 2\overline{\boldsymbol{G}}^{\mathrm{T}}\left[\overline{\boldsymbol{M}}_{\widetilde{x}\widetilde{\psi}}\left(\dot{\boldsymbol{\zeta}}\otimes\boldsymbol{I}\right) + \left(\boldsymbol{\zeta}\otimes\boldsymbol{I}\right)^{\mathrm{T}}\overline{\boldsymbol{M}}_{\widetilde{\psi}\psi}\left(\dot{\boldsymbol{\zeta}}\otimes\boldsymbol{I}\right)\right]\overline{\boldsymbol{\omega}} \\ &- \underbrace{\overline{\boldsymbol{G}}\mathrm{T}\left[\overline{\boldsymbol{\Theta}}_{\mathrm{u}} + \overline{\boldsymbol{M}}_{\widetilde{x}\widetilde{\psi}}\left(\boldsymbol{\zeta}\otimes\boldsymbol{I}\right) + \left(\boldsymbol{\zeta}\otimes\boldsymbol{I}\right)^{\mathrm{T}}\overline{\boldsymbol{M}}^{\mathrm{T}}_{\widetilde{x}\widetilde{\psi}} + \left(\boldsymbol{\zeta}\otimes\boldsymbol{I}\right)^{\mathrm{T}}\overline{\boldsymbol{M}}_{\widetilde{\psi}\widetilde{\psi}}\left(\boldsymbol{\zeta}\otimes\boldsymbol{I}\right)\right]\dot{\overline{\boldsymbol{G}}}\dot{\boldsymbol{\theta}}}_{\text{null if Euler parameters are used [31]}},\end{aligned} \tag{122}$$

$$\begin{aligned}\widehat{\boldsymbol{Q}}_{\mathrm{v_f}} =& \left(\boldsymbol{I}_{\zeta}\otimes\overline{\boldsymbol{\omega}}\right)^{\mathrm{T}}\left[\overline{\boldsymbol{M}}^{\mathrm{T}}_{\widetilde{x}\widetilde{\psi}} + \overline{\boldsymbol{M}}_{\widetilde{\psi}\psi}\left(\boldsymbol{\zeta}\otimes\boldsymbol{I}\right)\right]\overline{\boldsymbol{\omega}} + 2\overline{\boldsymbol{M}}^{\mathrm{T}}_{\widetilde{\psi}\psi}\left(\dot{\boldsymbol{\zeta}}\otimes\boldsymbol{I}\right)\overline{\boldsymbol{\omega}} \\ &+ \underbrace{\left[\overline{\boldsymbol{M}}^{\mathrm{T}}_{\widetilde{x}\psi} + \overline{\boldsymbol{M}}^{\mathrm{T}}_{\widetilde{\psi}\psi}\left(\boldsymbol{\zeta}\otimes\boldsymbol{I}\right)\right]\dot{\overline{\boldsymbol{G}}}\dot{\boldsymbol{\theta}}}_{\text{null if Euler parameters are used [31]}}.\end{aligned} \tag{123}$$

Note that $\dot{\overline{\boldsymbol{G}}}\dot{\boldsymbol{\theta}} = \boldsymbol{0}_{3\times 1}$, if Euler paramters are used [31].

2.3.5 Nodal-based absolute coordinate formulation

From our previous treatment of the FFRF it is clear that expressing the nodal positions relative to a moving frame leads to complex inertia forces. The ACF, initially proposed by [84] via the linearization of the strain tensor with respect to a corotated frame, eliminates this issue by employing directly the global nodal displacements to describe the configuration of the flexible body, i.e.,

$$\boldsymbol{q} = \boldsymbol{c}, \tag{124}$$

where, as already mentioned in Eq. (36), $\boldsymbol{c}$ includes rigid body translation, rigid body rotation, and flexible deformation. Hence,

$$\boldsymbol{r} = \boldsymbol{x}_{\mathrm{ref}} + \boldsymbol{c}, \tag{125}$$

and the coordinate Jacobian follows trivially as

$$\boldsymbol{L} = \boldsymbol{I}_{3n_{\mathrm{n}}\times 3n_{\mathrm{n}}}, \tag{126}$$

since $\boldsymbol{x}_{\mathrm{ref}} = \mathrm{const.}$; this leads to no quadratic velocity vector, since

$$\dot{\boldsymbol{L}} = \boldsymbol{0}_{3n_{\mathrm{n}}\times 3n_{\mathrm{n}}}. \tag{127}$$

Due to the fact that global coordinates are used to describe the body's motion, the inertia forces take a simple form, but not the elastic forces, since

$$\overline{\boldsymbol{c}}_{\mathrm{f}} = \boldsymbol{A}^{\mathrm{T}}_{\mathrm{bd}}\left(\boldsymbol{c} - \boldsymbol{c}_{\mathrm{rbm}}\right) \tag{128}$$

where

$$\boldsymbol{c}_{\mathrm{rbm}}\left(\boldsymbol{c}\right) = \boldsymbol{c}_{\mathrm{t}}\left(\boldsymbol{c}\right) + \boldsymbol{c}_{\mathrm{r}}\left(\boldsymbol{A}\left(\boldsymbol{c}\right)\right), \tag{129}$$

and

$$\boldsymbol{A}_{\mathrm{bd}} = \boldsymbol{A}_{\mathrm{bd}}(\boldsymbol{A}(\boldsymbol{c})), \tag{130}$$

since no rotation parameters are used as generalized coordinates in the ACF. However, there are several possibilities[14] to obtain the rigid body motion from the global displacement field, see, e.g., [84, 87]. We simply use $\boldsymbol{c}_{\mathrm{rbm}}$ and $\boldsymbol{A}_{\mathrm{bd}}$ for further considerations implying that these quantities are expressed explicitly in terms of $\boldsymbol{c}$.

[14] For example, the rigid body translation may be calculated as the average of the global displacement field and the rigid body rotation is associated with the average gradient of the global displacement field or may be calculated from the position of three points which may not lie on a line.

Hence[15],

$$\boldsymbol{P} = \frac{\partial \boldsymbol{A}_{\mathrm{bd}}^{\mathrm{T}}}{\partial \boldsymbol{c}} \left(\boldsymbol{c} - \boldsymbol{c}_{\mathrm{rbm}} \right) + \boldsymbol{A}_{\mathrm{bd}}^{\mathrm{T}} \left(\boldsymbol{I}_{3n_{\mathrm{n}} \times 3n_{\mathrm{n}}} - \frac{\partial \boldsymbol{c}_{\mathrm{rbm}}}{\boldsymbol{c}} \right). \tag{132}$$

Note that the virtual elastic work done by rigid body displacements is zero – rigid body displacements cannot give rise to internal forces, i.e.,

$$\boldsymbol{c}_{\mathrm{f}}^{\mathrm{T}} \boldsymbol{A}_{\mathrm{bd}} \overline{\boldsymbol{K}} \boldsymbol{A}_{\mathrm{bd}}^{\mathrm{T}} \delta \boldsymbol{c}_{\mathrm{rbm}} = \boldsymbol{c}_{\mathrm{f}}^{\mathrm{T}} \boldsymbol{A}_{\mathrm{bd}} \overline{\boldsymbol{K}} \boldsymbol{A}_{\mathrm{bd}}^{\mathrm{T}} \frac{\partial \boldsymbol{c}_{\mathrm{rbm}}}{\partial \boldsymbol{c}} \delta \boldsymbol{c} = 0, \tag{133}$$

which must hold for any virtual displacement, and, therefore, implies that $\left(\text{given } \overline{\boldsymbol{K}} = \overline{\boldsymbol{K}}^{\mathrm{T}}\right)$

$$\boldsymbol{c}_{\mathrm{f}}^{\mathrm{T}} \boldsymbol{A}_{\mathrm{bd}} \overline{\boldsymbol{K}} \boldsymbol{A}_{\mathrm{bd}}^{\mathrm{T}} \frac{\partial \boldsymbol{c}_{\mathrm{rbm}}}{\partial \boldsymbol{c}} = \boldsymbol{0}_{1 \times 3n_{\mathrm{n}}} \quad \overset{\text{transpose}}{\Leftrightarrow} \quad \frac{\partial \boldsymbol{c}_{\mathrm{rbm}}}{\partial \boldsymbol{c}^{\mathrm{T}}} \boldsymbol{A}_{\mathrm{bd}} \overline{\boldsymbol{K}} \boldsymbol{A}_{\mathrm{bd}}^{\mathrm{T}} \boldsymbol{c}_{\mathrm{f}} = \boldsymbol{0}_{3n_{\mathrm{n}} \times 1}, \tag{134}$$

which means there is no need to take the last term in Eq. (132) in the equations of motion into account. Hence, we find

$$\overline{\boldsymbol{M}} \ddot{\boldsymbol{c}} + \boldsymbol{A}_{\mathrm{bd}} \overline{\boldsymbol{K}} \boldsymbol{A}_{\mathrm{bd}}^{\mathrm{T}} \left(\boldsymbol{c} - \boldsymbol{c}_{\mathrm{rbm}} \right) + \left(\boldsymbol{c} - \boldsymbol{c}_{\mathrm{rbm}} \right)^{\mathrm{T}} \frac{\partial \boldsymbol{A}_{\mathrm{bd}}}{\partial \boldsymbol{c}^{\mathrm{T}}} \overline{\boldsymbol{K}} \boldsymbol{A}_{\mathrm{bd}}^{\mathrm{T}} \left(\boldsymbol{c} - \boldsymbol{c}_{\mathrm{rbm}} \right) + \frac{\partial \boldsymbol{g}}{\partial \boldsymbol{c}^{\mathrm{T}}} \boldsymbol{\lambda} = \boldsymbol{f}, \tag{135}$$

and the evaluation of the derivative of the rotation matrix with respect to the nodal displacements depends on the method used to obtain the rigid body motion from the global displacement field, as already discussed. Note that Eq. (135) agrees with the equations of motion proposed in [84], where a more traditional derivation is presented.

2.3.6 Nodal-based generalized component mode synthesis

The idea behind the GCMS is (i) to define a reduction basis, i.e., modes, that can represent large rigid body translation and rotation as well as flexible deformation for any given body orientation; and (ii) to obtain a linear relationship between the global finite element nodal displacements and the generalized coordinates.

To obtain the desired reduction matrix and generalized coordinates, we resort once again to the fundamental kinematic relationship stated in Eq. (42), where we can now restructure the matrix multiplications of the rigid body rotation and flexible part via Kronecker's product. In general [109],

$$\boldsymbol{u} = \boldsymbol{W}\boldsymbol{v} \in \mathbb{R}^{3\times 3} \quad \Rightarrow \quad \boldsymbol{u} = \left(\boldsymbol{v}^{\mathrm{T}} \otimes \boldsymbol{I} \right) \mathrm{vec}(\boldsymbol{W}) \in \mathbb{R}^{3\times 3}, \tag{136}$$

which can be applied to the nodal structure of Eq. (42); the rigid body rotation part may be written as (see also [89] for more details)

$$\boldsymbol{A}_{\mathrm{bd}} \overline{\boldsymbol{x}} = \left(\overline{\boldsymbol{X}} \otimes \boldsymbol{I} \right) \mathrm{vec}\left(\boldsymbol{A} \right), \tag{137}$$

where

$$\overline{\boldsymbol{X}} = \begin{bmatrix} \overline{\boldsymbol{x}}^{(1)^{\mathrm{T}}} \\ \vdots \\ \overline{\boldsymbol{x}}^{(n_{\mathrm{n}})^{\mathrm{T}}} \end{bmatrix} \in \mathbb{R}^{n_{\mathrm{n}} \times 3}, \tag{138}$$

are the nodal reference positions with respect to the floating frame slightly rearranged, and

$$\mathrm{vec}\left(\boldsymbol{A} \right) = \begin{bmatrix} A_{11} & A_{21} & A_{31} & A_{12} & A_{22} & A_{32} & A_{13} & A_{23} & A_{33} \end{bmatrix}^{\mathrm{T}}. \tag{139}$$

Likewise, the flexible part of Eq. (42) may be written as (again, see also [89] for more details)

$$\boldsymbol{A}_{\mathrm{bd}} \overline{\boldsymbol{\Psi}} \boldsymbol{\zeta} = \left(\overline{\boldsymbol{\Upsilon}} \otimes \boldsymbol{I} \right) \left(\boldsymbol{\zeta} \otimes \mathrm{vec}\left(\boldsymbol{A} \right) \right) \tag{140}$$

[15] Note that in general,

$$\frac{\partial \boldsymbol{T}}{\partial \boldsymbol{u}} \boldsymbol{v} = \begin{bmatrix} \frac{\partial \boldsymbol{T}}{\partial u_1} \boldsymbol{v} & \cdots & \frac{\partial \boldsymbol{T}}{\partial u_n} \boldsymbol{v} \end{bmatrix}. \tag{131}$$

where

$$\overline{\boldsymbol{\Upsilon}} = \begin{bmatrix} \overline{\boldsymbol{\psi}}_1^{(1)^{\mathrm{T}}} & \dots & \overline{\boldsymbol{\psi}}_{n_{\mathrm{m}}}^{(1)^{\mathrm{T}}} \\ \vdots & \dots & \vdots \\ \overline{\boldsymbol{\psi}}_1^{(n_{\mathrm{n}})^{\mathrm{T}}} & \dots & \overline{\boldsymbol{\psi}}_{n_{\mathrm{m}}}^{(n_{\mathrm{n}})^{\mathrm{T}}} \end{bmatrix} \in \mathbb{R}^{n_{\mathrm{n}} \times 3n_{\mathrm{m}}} \tag{141}$$

contains just all modes included in the reduction basis arranged according to Eq. (138). Hence,

$$\boldsymbol{r} = \boldsymbol{\Phi}\boldsymbol{q} \tag{142}$$

with

$$\boldsymbol{q} = \begin{bmatrix} \boldsymbol{\tau} \\ \mathrm{vec}\,(\boldsymbol{A}) \\ \boldsymbol{\zeta} \otimes \mathrm{vec}\,(\boldsymbol{A}) \end{bmatrix}, \tag{143}$$

and

$$\boldsymbol{\Phi} = \begin{bmatrix} (\mathbf{1} \otimes \boldsymbol{I}) & \left(\overline{\boldsymbol{X}} \otimes \boldsymbol{I}\right) & \left(\overline{\boldsymbol{\Upsilon}} \otimes \boldsymbol{I}\right) \end{bmatrix}, \tag{144}$$

where we see from Eq. (143) that the linear relationship between the global nodal positions[16] and the generalized coordinates is obtained at the expense of a nine-fold increase in the number of flexible modal coordinates, i.e., nine generalized flexible coordinates per original component mode of the bodies in the system.

The just derived linear relationship yields simple inertia forces, similar as in the ACF, since

$$\boldsymbol{L} = \boldsymbol{\Phi} = \mathrm{const.} \tag{145}$$

and

$$\dot{\boldsymbol{L}} = \mathbf{0}_{3n_{\mathrm{n}} \times (12+9n_{\mathrm{m}})}. \tag{146}$$

To obtain the coordinate mapping for the elastic forces we resort to Eqs. (142) to (144) and realize that

$$\boldsymbol{r}_{\mathrm{rbm}} = \boldsymbol{\Phi}\boldsymbol{q}_{\mathrm{rbm}} \tag{147}$$

with

$$\boldsymbol{q}_{\mathrm{rbm}} = \begin{bmatrix} \boldsymbol{\tau} \\ \mathrm{vec}\,(\boldsymbol{A}^*) \\ \mathbf{0}_{9n_{\mathrm{m}} \times 1} \end{bmatrix} \tag{148}$$

where $\mathrm{vec}\,(\boldsymbol{A}^*)$ denotes proper rotational coordinates obtained from $\mathrm{vec}\,(\boldsymbol{A})$ by an appropriate orthonormalization procedure and is therefore a function of $\mathrm{vec}\,(\boldsymbol{A})$ and no additional generalized coordinates are introduced here. To understand this it is important to mention that conventionally GCMS does not enforce the orthogonality condition during simulation, i.e., $\mathrm{vec}\,(\boldsymbol{A})$ does not necessarily refer to an orthogonal rotation matrix, which means $\mathrm{vec}\,(\boldsymbol{A})$ may also contain stretch and shear deformations, see [89]. Hence,

$$\overline{\boldsymbol{c}}_{\mathrm{f}}(\boldsymbol{q}) = \boldsymbol{\Phi}\widehat{\boldsymbol{A}}_{\mathrm{bd}}^{\mathrm{T}}\left(\boldsymbol{q} - \boldsymbol{q}_{\mathrm{rbm}}\right) \tag{149}$$

since

$$\boldsymbol{A}_{\mathrm{bd}}^{\mathrm{T}}\boldsymbol{\Phi} = \boldsymbol{\Phi}\widehat{\boldsymbol{A}}_{\mathrm{bd}}^{\mathrm{T}}. \tag{150}$$

The matrices in the previous equation commute[17], since the reduction matrix $\boldsymbol{\Phi}$ consists of blocks that are multiples of the identity matrix, see Eq. (144). Hence[18],

$$\boldsymbol{P} = \boldsymbol{\Phi}\frac{\partial \widehat{\boldsymbol{A}}_{\mathrm{bd}}^{\mathrm{T}}}{\partial \boldsymbol{q}}\left(\boldsymbol{q} - \boldsymbol{q}_{\mathrm{rbm}}\right) + \boldsymbol{\Phi}\widehat{\boldsymbol{A}}_{\mathrm{bd}}^{\mathrm{T}}\left(\boldsymbol{I}_{(12+9n_{\mathrm{m}})\times(12+9n_{\mathrm{m}})} - \frac{\partial \boldsymbol{q}_{\mathrm{rbm}}}{\boldsymbol{q}}\right). \tag{151}$$

[16] Note that originally Eq. (142) was proposed in terms of nodal displacements instead of positions in the GCMS.

[17] Note, the size of $\boldsymbol{A}_{\mathrm{bd}} \in \mathbb{R}^{3n_{\mathrm{n}} \times 3n_{\mathrm{n}}}$ changes to $\widehat{\boldsymbol{A}}_{\mathrm{bd}} \in \mathbb{R}^{(12+9n_{\mathrm{m}})\times(12+9n_{\mathrm{m}})}$ if the order of multiplication is changed, such that a proper matrix multiplication is well defined, i.e., matching dummy indices.

[18] Note, again, that in general,

$$\frac{\partial \boldsymbol{T}}{\partial \boldsymbol{u}}\boldsymbol{v} = \begin{bmatrix} \frac{\partial \boldsymbol{T}}{\partial u_1}\boldsymbol{v} & \dots & \frac{\partial \boldsymbol{T}}{\partial u_n}\boldsymbol{v} \end{bmatrix}.$$

Again, the virtual elastic work done by rigid body motion is zero; the last term of Eq. (151) does not need to be taken into account in the equations of motion, as before, see the ACF section. Hence, the final equations of motion, which agree with [88], are obtained as

$$\boldsymbol{\Phi}^{\mathrm{T}}\overline{\boldsymbol{M}}\boldsymbol{\Phi}\ddot{\boldsymbol{q}} + \widehat{\boldsymbol{A}}_{\mathrm{bd}}\boldsymbol{\Phi}^{\mathrm{T}}\overline{\boldsymbol{K}}\boldsymbol{\Phi}\widehat{\boldsymbol{A}}_{\mathrm{bd}}^{\mathrm{T}}\left(\boldsymbol{q}-\boldsymbol{q}_{\mathrm{rbm}}\right) + \left(\boldsymbol{q}-\boldsymbol{q}_{\mathrm{rbm}}\right)^{\mathrm{T}}\frac{\partial\widehat{\boldsymbol{A}}_{\mathrm{bd}}}{\partial\boldsymbol{q}^{\mathrm{T}}}\boldsymbol{\Phi}^{\mathrm{T}}\overline{\boldsymbol{K}}\boldsymbol{\Phi}\widehat{\boldsymbol{A}}_{\mathrm{bd}}^{\mathrm{T}}\left(\boldsymbol{q}-\boldsymbol{q}_{\mathrm{rbm}}\right) + \boldsymbol{J}^{\mathrm{T}}\boldsymbol{\lambda} = \boldsymbol{\Phi}^{\mathrm{T}}\boldsymbol{f}, \tag{152}$$

where the derivative of the rotation matrix with respect to the generalized coordinates contains zeros and ones only, see Eq. (143).

2.3.7 Nodal-based flexible natural coordinates formulation

The FNCF introduced by [94] can be interpreted as an extension of GCMS. The idea is to eliminate the non-linearity in GCMS's elastic forces by augmenting the generalized coordinates with the modal coordinates $\boldsymbol{\zeta}$, i.e.,

$$\boldsymbol{q} = \begin{bmatrix} \boldsymbol{\tau} \\ \mathrm{vec}\left(\boldsymbol{A}\right) \\ \boldsymbol{\zeta}\otimes\mathrm{vec}\left(\boldsymbol{A}\right) \\ \boldsymbol{\zeta} \end{bmatrix}, \tag{153}$$

where we see a ten-fold increase in modal coordinates compared to the nine-fold increase for GCMS. Hence,

$$\boldsymbol{r} = \boldsymbol{\Phi}^{*}\boldsymbol{q} \tag{154}$$

where

$$\boldsymbol{\Phi} = \begin{bmatrix}(\boldsymbol{1}\otimes\boldsymbol{I}) & \left(\overline{\boldsymbol{X}}\otimes\boldsymbol{I}\right) & \left(\overline{\boldsymbol{\Upsilon}}\otimes\boldsymbol{I}\right) & \boldsymbol{0}_{3n_{\mathrm{n}}\times n_{\mathrm{m}}}\end{bmatrix}. \tag{155}$$

This specific choice of generalized coordinates yields linear inertia terms as in GCMS, i.e.,

$$\boldsymbol{L} = \boldsymbol{\Phi}^{*} = \mathrm{const.}, \tag{156}$$

and

$$\dot{\boldsymbol{L}} = \boldsymbol{0}_{3n_{\mathrm{n}}\times(12+10n_{\mathrm{m}})}. \tag{157}$$

The augmentation of the generalized coordinates enables the extraction of the flexible nodal-displacements from the generalized coordinates with a Boolean matrix and the reduction basis in a similar manner as in CMS-FFRF, i.e.,

$$\overline{\boldsymbol{c}}_{\mathrm{f}} = \overline{\boldsymbol{\Psi}}\boldsymbol{B}^{*}\boldsymbol{q} \tag{158}$$

with

$$\boldsymbol{B}^{*} = \begin{bmatrix}\boldsymbol{0}_{3n_{\mathrm{n}}\times 3} & \boldsymbol{0}_{3n_{\mathrm{n}}\times 9} & \boldsymbol{0}_{3n_{\mathrm{n}}\times 9n_{\mathrm{m}}} & \boldsymbol{I}_{3n_{\mathrm{n}}\times n_{\mathrm{m}}}\end{bmatrix}. \tag{159}$$

Hence, the corresponding coordinate Jacobian follows as

$$\boldsymbol{P} = \overline{\boldsymbol{\Psi}}\boldsymbol{B}^{*}. \tag{160}$$

Finally, the equations of motion simply read

$$\boldsymbol{\Phi}^{*\mathrm{T}}\overline{\boldsymbol{M}}\boldsymbol{\Phi}^{*}\ddot{\boldsymbol{q}} + \boldsymbol{B}^{*\mathrm{T}}\overline{\boldsymbol{\Psi}}^{\mathrm{T}}\overline{\boldsymbol{K}}\,\overline{\boldsymbol{\Psi}}\boldsymbol{B}^{*}\boldsymbol{q} + \boldsymbol{J}^{\mathrm{T}}\boldsymbol{\lambda} = \boldsymbol{\Phi}^{*\mathrm{T}}\boldsymbol{f}, \tag{161}$$

but are subjected to $9n_{\mathrm{m}} + 6$ reference constraints to eliminate the coordinate redundancy in the generalized coordinates, see Eq. (153), and to enforce the orthogonality condition of the rotation matrix – in contrast to GCMS where conventionally no reference constraints are enforced with additional Lagrange multipliers.

It should be emphasized that originally [94] the FNCF was proposed with a lumped mass approximation in contrast to the consistent mass approach presented in the present paper, although, the structure of the equations is exactly the same.

2.3.8 Overview of nodal-based formulations

Tab. 1 depicts the ingredients of the formulations derived with the unified framework (see also the summary at the end of Sect. 2.3.2) presented in the current paper[19]. Comparing ACF and FFRF shows that absolute coordinates yield simple inertia forces but complex elastic forces, whereas local coordinates yield complex inertia forces but simple elastic forces. It is also clear that successively increasing the number of generalized coordinates – a nine-fold and ten-fold increase in the number of modal coordinates in GCMS and FNCF, respectively – yields a simpler structure of the governing equations of motion, with the extreme case being FNCF, where the significant increase in generalized coordinates requires in addition $9m + 6$ reference constraints to eliminate coordinate redundancies, but results in linear equations of motion.

Summary of the main result of Sect. 2.3.3 to Sect. 2.3.8 – overview of the formulations derived with the unified framework

Table 1: Equation of motion ingredients of the formulations derived with the unified framework presented in the current paper; the generic equations presented in Eq. (78) are reprinted here for presentation purposes, i.e.,

$$\boldsymbol{L}^{\mathrm{T}}\overline{\boldsymbol{M}}\boldsymbol{L}\ddot{\boldsymbol{q}} + \boldsymbol{L}^{\mathrm{T}}\overline{\boldsymbol{M}}\dot{\boldsymbol{L}}\dot{\boldsymbol{q}} + \boldsymbol{P}^{\mathrm{T}}\overline{\boldsymbol{K}}\overline{\boldsymbol{c}}_{\mathrm{f}}(\boldsymbol{q}) + \boldsymbol{J}^{\mathrm{T}}\boldsymbol{\lambda} = \boldsymbol{L}^{\mathrm{T}}\boldsymbol{f}$$

with the coordinate and constraint Jacobians

$$\boldsymbol{L} = \frac{\partial \boldsymbol{r}}{\partial \boldsymbol{q}}, \quad \boldsymbol{P} = \frac{\partial \overline{\boldsymbol{c}}_{\mathrm{f}}}{\partial \boldsymbol{q}}, \quad \boldsymbol{J} = \frac{\partial \boldsymbol{g}}{\partial \boldsymbol{q}},$$

see also the summary at the end of Sect. 2.3.2.

EOMs	ACF	CMS-FFRF	GCMS	FNCF
$\boldsymbol{q}$	$\boldsymbol{c}$	$\begin{bmatrix}\boldsymbol{\tau}^{\mathrm{T}} & \boldsymbol{\theta}^{\mathrm{T}} & \boldsymbol{\zeta}^{\mathrm{T}}\end{bmatrix}^{\mathrm{T}}$	$\begin{bmatrix}\boldsymbol{\tau}^{\mathrm{T}} & \mathrm{vec}(\boldsymbol{A})^{\mathrm{T}} & (\boldsymbol{\zeta}\otimes\mathrm{vec}(\boldsymbol{A}))^{\mathrm{T}}\end{bmatrix}^{\mathrm{T}}$	$\begin{bmatrix}\boldsymbol{\tau}^{\mathrm{T}} & \mathrm{vec}(\boldsymbol{A})^{\mathrm{T}} & (\boldsymbol{\zeta}\otimes\mathrm{vec}(\boldsymbol{A}))^{\mathrm{T}} & \boldsymbol{\zeta}^{\mathrm{T}}\end{bmatrix}^{\mathrm{T}}$
$\boldsymbol{r}(\boldsymbol{q})$	$\boldsymbol{x}_{\mathrm{ref}} + \boldsymbol{c}$	$(\boldsymbol{1}\otimes\boldsymbol{I})\boldsymbol{\tau} + \boldsymbol{A}_{\mathrm{bd}}\overline{\boldsymbol{x}} + \boldsymbol{A}_{\mathrm{bd}}\overline{\boldsymbol{\Psi}}\boldsymbol{\zeta}$	$(\boldsymbol{1}\otimes\boldsymbol{I})\boldsymbol{\tau} + \left(\overline{\boldsymbol{X}}\otimes\boldsymbol{I}\right)\mathrm{vec}(\boldsymbol{A}) + \left(\overline{\boldsymbol{\Upsilon}}\otimes\boldsymbol{I}\right)(\boldsymbol{\zeta}\otimes\mathrm{vec}(\boldsymbol{A}))$	$(\boldsymbol{1}\otimes\boldsymbol{I})\boldsymbol{\tau} + \left(\overline{\boldsymbol{X}}\otimes\boldsymbol{I}\right)\mathrm{vec}(\boldsymbol{A}) + \left(\overline{\boldsymbol{\Upsilon}}\otimes\boldsymbol{I}\right)(\boldsymbol{\zeta}\otimes\mathrm{vec}(\boldsymbol{A}))$
$\boldsymbol{L}$	$\boldsymbol{I}_{3n_{\mathrm{n}}\times 3n_{\mathrm{n}}}$	$\begin{bmatrix}(\boldsymbol{1}\otimes\boldsymbol{I}) & -\boldsymbol{A}_{\mathrm{bd}}\widetilde{\overline{\boldsymbol{r}}}_{\mathrm{f}}\overline{\boldsymbol{G}} & \boldsymbol{A}_{\mathrm{bd}}\overline{\boldsymbol{\Psi}}\end{bmatrix}$	$\begin{bmatrix}(\boldsymbol{1}\otimes\boldsymbol{I}) & \left(\overline{\boldsymbol{X}}\otimes\boldsymbol{I}\right) & \left(\overline{\boldsymbol{\Upsilon}}\otimes\boldsymbol{I}\right)\end{bmatrix}$	$\begin{bmatrix}(\boldsymbol{1}\otimes\boldsymbol{I}) & \left(\overline{\boldsymbol{X}}\otimes\boldsymbol{I}\right) & \left(\overline{\boldsymbol{\Upsilon}}\otimes\boldsymbol{I}\right) & \boldsymbol{0}_{3n_{\mathrm{n}}\times n_{\mathrm{m}}}\end{bmatrix}$
$\dot{\boldsymbol{L}}$	$\boldsymbol{0}_{3n_{\mathrm{n}}\times 3n_{\mathrm{n}}}$	$\begin{bmatrix}\boldsymbol{0}_{3n_{\mathrm{n}}\times 3} & -\boldsymbol{A}_{\mathrm{bd}}\left(\widetilde{\overline{\boldsymbol{\omega}}}_{\mathrm{bd}}\widetilde{\overline{\boldsymbol{r}}}_{\mathrm{f}}\overline{\boldsymbol{G}} + \widetilde{\dot{\overline{\boldsymbol{c}}}}_{\mathrm{f}}\overline{\boldsymbol{G}} + \widetilde{\overline{\boldsymbol{r}}}_{\mathrm{f}}\dot{\overline{\boldsymbol{G}}}\right) & \boldsymbol{A}_{\mathrm{bd}}\widetilde{\overline{\boldsymbol{\omega}}}_{\mathrm{bd}}\overline{\boldsymbol{\Psi}}\end{bmatrix}$	$\boldsymbol{0}_{3n_{\mathrm{n}}\times(12+9n_{\mathrm{m}})}$	$\boldsymbol{0}_{3n_{\mathrm{n}}\times(12+10n_{\mathrm{m}})}$
$\overline{\boldsymbol{c}}_{\mathrm{f}}(\boldsymbol{q})$	$\boldsymbol{A}_{\mathrm{bd}}^{\mathrm{T}}\left(\boldsymbol{c} - \boldsymbol{c}_{\mathrm{rbm}}\right)$	$\overline{\boldsymbol{\Psi}}\boldsymbol{B}\boldsymbol{q}$	$\boldsymbol{L}\widehat{\boldsymbol{A}}_{\mathrm{bd}}^{\mathrm{T}}\left(\boldsymbol{q} - \boldsymbol{q}_{\mathrm{rbm}}\right)$	$\overline{\boldsymbol{\Psi}}\boldsymbol{B}^{*}\boldsymbol{q}$
$\boldsymbol{P}$	$\frac{\partial \boldsymbol{A}_{\mathrm{bd}}^{\mathrm{T}}}{\partial \boldsymbol{c}}\boldsymbol{c}_{\mathrm{f}} + \boldsymbol{A}_{\mathrm{bd}}^{\mathrm{T}}\left(\boldsymbol{I}_{3n_{\mathrm{n}}\times 3n_{\mathrm{n}}} - \frac{\partial \boldsymbol{c}_{\mathrm{rbm}}}{\boldsymbol{c}}\right)$	$\overline{\boldsymbol{\Psi}}\boldsymbol{B}$	$\boldsymbol{L}\frac{\partial \widehat{\boldsymbol{A}}_{\mathrm{bd}}^{\mathrm{T}}}{\partial \boldsymbol{q}}\left(\boldsymbol{q} - \boldsymbol{q}_{\mathrm{rbm}}\right) + \boldsymbol{L}\widehat{\boldsymbol{A}}_{\mathrm{bd}}^{\mathrm{T}}\left(\boldsymbol{I}_{(12+9n_{\mathrm{m}})\times(12+9n_{\mathrm{m}})} - \frac{\partial \boldsymbol{q}_{\mathrm{rbm}}}{\partial \boldsymbol{q}}\right)$	$\overline{\boldsymbol{\Psi}}\boldsymbol{B}^{*}$

[19] Note that the FFRF without modal reduction is not included in the table for lack of space, however, the ingredients are the same with the exception that $\overline{\boldsymbol{\Psi}}\boldsymbol{\zeta}$ is replaced by $\overline{\boldsymbol{c}}_{\mathrm{f}}$.

3 Conclusion

Corotational flexible multibody dynamics formulations are based on a kinematic description that additively decomposes the total displacement field of a linearly-elastic flexible body into an arbitrarily large rigid body motion and superimposed small deformations. The importance of corotational formulations is induced by their suitability to model a variety of engineering systems of practical importance, efficiently. Furthermore, the idea of such a splitting of displacements into rigid body motion and deformation comes naturally, is intuitive, i.e., a straightforward extension of rigid body dynamics, and easy to implement and extend. Therefore, corotational formulations attract researchers as well as practitioners in academia and industry. Even though that these assumptions of corotationally-linearized strains remain the same, various formulations have evolved and may be found in several review papers and textbooks referenced in this contribution.

The mainstream approach employing local flexible generalized coordinates is identified as the floating frame of reference formulation and is based on an integral view of continuously interpolated domains and a lumped mass approximation to enable practical computer implementations without access to the algorithmic level of the finite element code.

As an extension of the existing literature, a unification framework is proposed, using a small set of quantities and operations to concisely formulate the equations of motion for various state-of-the-art corotational flexible multibody dynamics formulations with significantly less effort. This, so-called, nodal-based, i.e., a priori space-wise discretized, view avoids impractical integrals and approximative lumped mass approaches, while still enabling the typical workflow of flexible multibody dynamics simulations (described in this paper) without access to the algorithmic level of the finite element code, and therefore, being fully compatible with standard multibody dynamics code infrastructure. This unified framework reduces the information and complexity within the scientific literature by clearly showing the equivalence of the presented formulations, i.e., the floating frame of reference formulation, the component mode synthesis floating frame of reference formulation, the absolute coordinate formulation, the generalized component mode synthesis, and the flexible natural coordinates formulation, and highlights the fact that the formulations differ only in the choice of generalized coordinates. The unification and simplification of the formulations should also allow researchers to develop both more efficient algorithms as well as more comprehensive extensions, e.g., in the areas of geometric nonlinearities, nonlinear material behavior, contact problems, model order reduction, etc.

Authors' Contributions

Andreas Zwölfer; development and derivation of the unified formulation framework; formulation of overarching research goals and aims; literature procurement; writing of Sections 1.1 to 1.6, 2, and 3; review and editing of final manuscript. Johannes Gerstmayr; contributed to some ideas of the unified formulation framework; formulation of overarching research goals and aims; literature procurement; writing of Sections 1.6 and 3; review and editing of final manuscript.

References

[1] A. Shabana. Flexible multibody dynamics: Review of past and recent developments. *Multibody system dynamics*, 1(2):189–222, 1997.

[2] T. Wasfy and A. Noor. Computational strategies for flexible multibody systems. *Applied Mechanics Reviews*, 56(6):553–613, 2003.

[3] O. A. Bauchau. *Flexible multibody dynamics*. Springer, 2011.

[4] R. L. Huston. Multi-body dynamics including the effects of flexibility and compliance. *Computers & Structures*, 14(5-6):443–451, 1981.

[5] R. L. Huston. Multibody dynamics – modeling and analysis methods. *Applied Mechanics Reviews*, 44(3):109–117, 1991.

[6] R. L. Huston. Computer methods in flexible multibody dynamics. *International Journal for Numerical Methods in Engineering*, 32(8):1657–1668, 1991.

[7] W. Schiehlen. Multibody system dynamics: Roots and perspectives. *Multibody System Dynamics*, 1:149–188, 1997.

[8] H. Bremer. On the dynamics of elastic multibody systems. *Applied Mechanics Reviews*, 52(9):275–303, 1999.

[9] P. Eberhard and W. Schiehlen. Computational dynamics of multibody systems: History, formalisms, and applications. *Journal of Computational and Nonlinear Dynamics*, 1(1):3–12, 2006.

[10] W. Schiehlen. Computational dynamics: theory and applications of multibody systems. *European Journal of Mechanics - A/Solids*, 25(4):566–594, 2006.

[11] O. A. Bauchau and A. Laulusa. Review of contemporary approaches for constraint enforcement in multibody systems. *Journal of Computational and Nonlinear Dynamics*, 3(1), 2008.

[12] J. Gerstmayr, H. Sugiyama, and A. Mikkola. Review on the absolute nodal coordinate formulation for large deformation analysis of multibody systems. *Journal of Computational and Nonlinear Dynamics*, 8(3):031016, 2013.

[13] Q. Tian, P. Flores, and H. M. Lankarani. A comprehensive survey of the analytical, numerical and experimental methodologies for dynamics of multibody mechanical systems with clearance or imperfect joints. *Mechanism and Machine Theory*, 122:1–57, 2018.

[14] B. Rong, X. Rui, L. Tao, and G. Wang. Theoretical modeling and numerical solution methods for flexible multibody system dynamics. *Nonlinear Dynamics*, 98(2):1519–1553, 2019.

[15] X. Rui, X. Wang, Q. Zhou, and J. Zhang. Transfer matrix method for multibody systems (rui method) and its applications. *Science China Technological Sciences*, 62(5):712–720, 2019.

[16] P. Flores. Contact mechanics for dynamical systems: a comprehensive review. *Multibody System Dynamics*, 54:127–177, 2021.

[17] V. Gufler, E. Wehrle, and A. Zwölfer. A review of flexible multibody dynamics for gradient-based design optimization. *Multibody System Dynamics*, 53:379–409, 2021.

[18] K. Otsuka, K. Makihara, and H. Sugiyama. Recent advances in the absolute nodal coordinate formulation: Literature review from 2012 to 2020. *Journal of Computational and Nonlinear Dynamics*, 17(8), 2022.

[19] R. L. Huston. *Multibody Dynamics*. Butterworth-Heinemann, 1990.

[20] H. Bremer and F. Pfeiffer. *Elastische Mehrkörpersysteme*. Teubner, 1992.

[21] J. G. D. Jalón and E. Bayo. *Kinematic and dynamic simulation of multibody systems: the real-time challenge*. Springer, 1994.

[22] R. Schwertassek and O. Wallrapp. *Dynamik flexibler Mehrkörpersysteme*. Grundlagen und Fortschritte der Ingenieurwissenschaften. Vieweg+Teubner, 1999.

[23] M. Géradin and A. Cardona. *Flexible Multibody Dynamics: A Finite Element Approach*. John Wiley & Sons, 2001.

[24] H. Bremer. *Elastic Multibody Dynamics*. Springer, 2008.

[25] F. Pfeiffer. *Mechanical system dynamics*. Springer, 2008.

[26] A. Jain. *Robot and Multibody Dynamics: Analysis and Algorithms*. Springer, 2011.

[27] B. Simeon. *Computational Flexible Multibody Dynamics: a differential-algebraic approach*. Springer, 2013.

[28] W. Schiehlen and P. Eberhard. *Applied dynamics*. Springer, 2014.

[29] R. Seifried. *Dynamics of underactuated multibody systems: modeling, control and optimal design*. Springer, 2014.

[30] A. A. Shabana. *Computational Continuum Mechanics*. John Wiley & Sons, 3rd edition, 2018.

[31] A. Shabana. *Dynamics of Multibody Systems*. Cambridge University Press, 5th edition, 2020.

[32] J. C. Simo and L. Vu-Quoc. On the Dynamics of Flexible Beams Under Large Overall Motions–The Plane Case: Part I. *Journal of Applied Mechanics*, 53(4):849–854, 1986.

[33] C. Felippa and B. Haugen. A unified formulation of small-strain corotational finite elements: I. theory. *Computer Methods in Applied Mechanics and Engineering*, 194(21-24):2285–2335, 2005.

[34] T. Belytschko and B. J. Hsieh. Non-linear transient finite element analysis with convected co-ordinates. *International Journal for Numerical Methods in Engineering*, 7(3):255–271, 1973.

[35] G. Wempner. Finite elements, finite rotations and small strains of flexible shells. *International Journal of Solids and Structures*, 5(2):117–153, 1969.

[36] B. Nour-Omid and C. Rankin. Finite rotation analysis and consistent linearization using projectors. *Computer Methods in Applied Mechanics and Engineering*, 93(3):353–384, 1991.

[37] R. de Borst, M. Crisfield, J. Remmers, and C. Verhoosel. *Nonlinear Finite Element Analysis of Solids and Structures*. John Wiley & Sons, 2nd edition, 2012.

[38] B. M. Fraeijs de Veubeke. The dynamics of flexible bodies. *International Journal of Engineering Science*, 14(10):895–913, 1976.

[39] C. Nowakowski, J. Fehr, M. Fischer, and P. Eberhard. Model order reduction in elastic multibody systems using the floating frame of reference formulation. *IFAC Proceedings Volumes*, 45(2):40–48, 2012.

[40] B. Besselink, U. Tabak, A. Lutowska, N. van de Wouw, H. Nijmeijer, et al. A comparison of model reduction techniques from structural dynamics, numerical mathematics and systems and control. *Journal of Sound and Vibration*, 332(19):4403–4422, 2013.

[41] V. Sonneville, M. Scapolan, M. Shan, and O. A. Bauchau. Modal reduction procedures for flexible multibody dynamics. *Multibody System Dynamics*, 51(4):377–418, 2021.

[42] M. C. C. Bampton and R. R. Craig Jr. Coupling of substructures for dynamic analyses. *AIAA Journal*, 6(7):1313–1319, 1968.

[43] W. C. Hurty. Dynamic analysis of structural systems using component modes. *AIAA Journal*, 3(4):678–685, 1965.

[44] B. Irons. Structural eigenvalue problems - elimination of unwanted variables. *AIAA Journal*, 3(5):961–962, 1965.

[45] S. Rubin. Improved component-mode representation for structural dynamic analysis. *AIAA Journal*, 13(8):995–1006, 1975.

[46] R. H. Macneal. A hybrid method of component mode synthesis. *Computers and Structures*, 1(4):581–601, 1971.

[47] M. Lehner and P. Eberhard. On the use of moment-matching to build reduced order models in flexible multibody dynamics. *Multibody System Dynamics*, 16:191–211, 2006.

[48] M. Lehner and P. Eberhard. A two-step approach for model reduction in flexible multibody dynamics. *Multibody System Dynamics*, 17:157–176, 2007.

[49] P. Korkealaakso, A. Mikkola, T. Rantalainen, and A. Rouvinen. Description of joint constraints in the floating frame of reference formulation. *Proceedings of the Institution of Mechanical Engineers, Part K: Journal of Multi-body Dynamics*, 223:133–145, 2009.

[50] A. Laulusa and O. A. Bauchau. Review of classical approaches for constraint enforcement in multibody systems. *Journal of Computational and Nonlinear Dynamics*, 3(1), 2007.

[51] S. Kim and E. Haug. A recursive formulation for flexible multibody dynamics, part I: open-loop systems. *Computer Methods in Applied Mechanics and Engineering*, 71:293–314, 1988.

[52] A. Jain and G. Rodriguez. Recursive flexible multibody system dynamics using spatial operators. *Journal of Guidance, Control, and Dynamics*, 15(6):1453–1466, 1992.

[53] S.-S. Kim and E. J. Haug. A recursive formulation for flexible multibody dynamics, part II: closed loop systems. *Computer Methods in Applied Mechanics and Engineering*, 74(3):251–269, 1989.

[54] Y. L. Hwang, A. A. Shabana, and R. A. Wehage. Projection methods in flexible multibody dynamics. part II: Dynamics and recursive projection methods. *International journal for numerical methods in engineering*, 35(10):1941–1966, 1992.

[55] A. A. Shabana, Y. L. Hwang, and R. A. Wehage. Projection methods in flexible multibody dynamics. part I: Kinematics. *International journal for numerical methods in engineering*, 35(10):1927–1939, 1992.

[56] G. H. K. Heirman and W. Desmet. Interface reduction of flexible bodies for efficient modeling of body flexibility in multibody dynamics. *Multibody System Dynamics*, 24(2):219–234, 2010.

[57] J.-G. Ahn, J.-G. Kim, and H.-I. Yang. Interpolation multipoint constraints with selection criteria of degree of freedoms for flexible multibody dynamics. *Applied Mathematics and Computation*, 409:126361, 2021.

[58] K. Sherif, K. Nachbagauer, and W. Steiner. On the rotational equations of motion in rigid body dynamics when using euler parameters. *Nonlinear Dynamics*, 81(1-2):343–352, 2015.

[59] R. Schwertassek, O. Wallrapp, and A. A. Shabana. Flexible multibody simulation and choice of shape functions. *Nonlinear Dynamics*, 20(4):361–380, 1999.

[60] J. Canavin and P. Likins. Floating reference frames for flexible spacecraft. *Journal of Spacecraft and Rockets*, 14(12):724–732, 1977.

[61] O. Agrawal and A. Shabana. Application of deformable-body mean axis to flexible multibody system dynamics. *Computer Methods in Applied Mechanics and Engineering*, 56(2):217–245, 1986.

[62] O. P. Agrawal and A. A. Shabana. Dynamic analysis of multibody systems using component modes. *Computers & Structures*, 21(6):1303–1312, 1985.

[63] A. Cammarata and C. Pappalardo. On the use of component mode synthesis methods for the model reduction of flexible multibody systems within the floating frame of reference formulation. *Mechanical Systems and Signal Processing*, 142:106745, 2020.

[64] A. Cammarata, R. Sinatra, and P. D. Maddìo. Interface reduction in flexible multibody systems using the floating frame of reference formulation. *Journal of Sound and Vibration*, 523:116720, 2022.

[65] A. Shabana and G. Wang. Durability analysis and implementation of the floating frame of reference formulation. *Proc IMechE Part K: Journal of Multi-body Dynamics*, 232(3):295–313, 2018.

[66] N. M. Newmark. A method of computation for structural dynamics. *ASCE Journal of the Engineering Mechanics Division*, 85 (3):67–94, 1959.

[67] H. M. Hilber, T. J. R. Hughes, and R. L. Taylor. Improved numerical dissipation for time integration algorithms in structural dynamics. *Earthquake Engineering & Structural Dynamics*, 5(3):283–292, 1977.

[68] J. Chung and G. M. Hulbert. A time integration algorithm for structural dynamics with improved numerical dissipation: The generalized-α method. *ASME Journal of Applied Mechanics*, 60(2):371–375, 1993.

[69] M. Arnold and O. Brüls. Convergence of the generalized-α scheme for constrained mechanical systems. *Multibody System Dynamics*, 18(2):185–202, 2007.

[70] O. Brüls, A. Cardona, and M. Arnold. Lie group generalized-α time integration of constrained flexible multibody systems. *Mechanism and Machine Theory*, 48:121–137, 2012.

[71] FunctionBay, Inc. *Recurdyn Online Help*, 2019. Accessed on Aug. 01, 2019. [Online]. Available: https://functionbay.com/documentation/onlinehelp/default.htm.

[72] MSC Software Corporation. *Theory of flexible bodies*, 2019. Adams/Flex documentation.

[73] Siemens Product Lifecycle Management Software Inc. *NX Help*, 2019. Accessed on Dec. 21, 2022. [Online]. Available: https://docs.plm.automation.siemens.com/tdoc/nx/1899/nx_help/.

[74] Altair Engineering Inc. *MotionSolve User and Refernce Guide*, 2022. Accessed on Dec. 21, 2022. [Online]. Available: https://2022.help.altair.com/2022/hwsolvers/ms/index.htm.

[75] SIMPACK. *SIMPACK Documentation*, 2013.

[76] K. Sherif and K. Nachbagauer. A detailed derivation of the velocity-dependent inertia forces in the floating frame of reference formulation. *Journal of Computational and Nonlinear Dynamics*, 9(4):044501, 2014.

[77] H. Irschik, M. Krommer, M. Nader, Y. Vetyukov, and H. Garssen. The equations of Lagrange for a continuous deformable body with rigid body degrees of freedom, written in a momentum based formulation. *Journal of Sound and Vibration*, 335:269–285, 2015.

[78] G. Orzechowski, M. K. Matikainen, and A. M. Mikkola. Inertia forces and shape integrals in the floating frame of reference formulation. *Nonlinear Dynamics*, 88(3):1953–1968, 2017.

[79] A. A. Shabana, G. Wang, and S. Kulkarni. Further investigation on the coupling between the reference and elastic displacements in flexible body dynamics. *Journal of Sound and Vibration*, 427:159–177, 2018.

[80] U. Lugrís, M. Naya, F. González, and J. Cuadrado. Performance and application criteria of two fast formulations for flexible multibody dynamics. *Mechanics Based Design of Structures and Machines*, 35(4):381–404, 2007.

[81] W. Witteveen and F. Pichler. On the relevance of inertia related terms in the equations of motion of a flexible body in the floating frame of reference formulation. *Multibody System Dynamics*, 46:77–105, 2019.

[82] W. Schiehlen. Research trends in multibody system dynamics. *Multibody System Dynamics*, 18:3–13, 2007.

[83] R. Vidoni, P. Gallina, P. Boscariol, A. Gasparetto, and M. Giovagnoni. Modeling the vibration of spatial flexible mechanisms through an equivalent rigid-link system/component mode synthesis approach. *Journal of Vibration and Control*, 23(12): 1890–1907, 2015.

[84] J. Gerstmayr and J. Schöberl. A 3d finite element method for flexible multibody systems. *Multibody System Dynamics*, 15(4): 305–320, 2006.

[85] J. Gerstmayr and J. Schöberl. A 3d finite element approach to flexible multibody systems. In H. Mang, F. Rammerstorfer, and J. Eberhardsteiner, editors, *Proceedings of the Fifth World Congress on Computational Mechanics (WCCM V)*, 2002.

[86] J. Gerstmayr. Strain tensors in the absolute nodal coordinate and the floating frame of reference formulation. *Nonlinear Dynamics*, 34:133–145, 2003.

[87] J. Gerstmayr and J. A. C. Ambrósio. Component mode synthesis with constant mass and stiffness matrices applied to flexible multibody systems. *International Journal for Numerical Methods in Engineering*, 73(11):1518–1546, 2008.

[88] A. Pechstein, D. Reischl, and J. Gerstmayr. A generalized component mode synthesis approach for flexible multibody systems with a constant mass matrix. *Journal of Computational and Nonlinear Dynamics*, 8(1):011019, 2013.

[89] A. Zwölfer and J. Gerstmayr. Preconditioning strategies for linear dependent generalized component modes in 3d flexible multibody dynamics. *Multibody System Dynamics*, 47:65–93, 2019.

[90] A. Zwölfer and J. Gerstmayr. Co-rotational formulations for 3D flexible multibody systems: A nodal-based approach. In H. Altenbach, H. Irschik, and V. P. Matveenko, editors, *Contributions to Advanced Dynamics and Continuum Mechanics*, pages 243–263. Springer, 2019.

[91] R. Winkler and J. Gerstmayr. A projection-based approach for the derivation of the floating frame of reference formulation for multibody systems. *Acta Mechanica*, 230(1):1–29, 2019.

[92] F. Naets, T. Devos, A. Humer, and J. Gerstmayr. A noninvasive system-level model order reduction scheme for flexible multibody simulation. *Int J Numer Methods Eng*, 121:3083–3107, 2020.

[93] O. Brüls, P. Duysinx, and J.-C. Golinval. The global modal parameterization for non-linear model-order reduction in flexible multibody dynamics. *International Journal for Numerical Methods in Engineering*, 69(5):948–977, 2007.

[94] M. Vermaut, F. Naets, and W. Desmet. A flexible natural coordinates formulation (FNCF) for the efficient simulation of small-deformation multibody systems. *International Journal for Numerical Methods in Engineering*, 115(11):1353–1370, 2018.

[95] A. Cardona and M. Géradin. Modelling of superelements in mechanism analysis. *International Journal for Numerical Methods in Engineering*, 32(8):1565–1593, 1991.

[96] A. Cardona and M. Géradin. A superelement formulation for mechanism analysis. *Computer Methods in Applied Mechanics and Engineering*, 100(1):1–29, 1992.

[97] A. Cardona. Superelements modelling in flexible multibody dynamics. *Multibody System Dynamics*, 4(2/3):245–266, 2000.

[98] M. Ellenbroek and J. Schilder. On the use of absolute interface coordinates in the floating frame of reference formulation for flexible multibody dynamics. *Multibody system dynamics*, 43:193–208, 2018.

[99] M. Géradin and D. Rixen. Impulse-based substructuring in a floating frame to simulate high frequency dynamics in flexible multibody dynamics. *Multibody system dynamics*, 42:47–77, 2018.

[100] M. Géradin and D. J. Rixen. Dynamics of a flexible body: a two-field formulation. *Multibody System Dynamics*, 54:1–29, 2021.

[101] M. Géradin and D. J. Rixen. A fresh look at the dynamics of a flexible body application to substructuring for flexible multibody dynamics. *International Journal for Numerical Methods in Engineering*, 122(14):3525–3582, 2021.

[102] A. Zwölfer and J. Gerstmayr. A concise nodal-based derivation of the floating frame of reference formulation for displacement-based solid finite elements: Avoiding inertia shape integrals. *Multibody System Dynamics*, 49:291–313, 2020.

[103] U. Lugrís, M. A. Naya, A. Luaces, and J. Cuadrado. Efficient calculation of the inertia terms in floating frame of reference formulations for flexible multibody dynamics. *Proceedings of the Institution of Mechanical Engineers, Part K: Journal of Multi-body Dynamics*, 223(2):147–157, 2009.

[104] A. Zwölfer and J. Gerstmayr. The nodal-based floating frame of reference formulation with modal reduction: How to calculate the invariants without a lumped mass approximation. *Acta Mechanica*, 232:835–851, 2021.

[105] O. Zienkiewicz and R. Taylor. *The Finite Element Method: The basis*, volume 1. Butterworth-Heinemann, 5th edition, 2000.

[106] C. A. Felippa. *INTRODUCTION to FINITE ELEMENT METHODS*. University of Colorado Boulder, 2003.

[107] K. Kim. A review of mass matrices for eigenproblems. *Computers & Structures*, 46(6):1041–1048, 1993.

[108] P. Tong, T. Pian, and L. Bucciarblli. Mode shapes and frequencies by finite element method using consistent and lumped masses. *Computers & Structures*, 1(4):623–638, 1971.

[109] A. Graham. *Kronecker products and matrix calculus with applications*. Dover Publications, 2018.